US012383162B2

(12) **United States Patent** (10) **Patent No.: US 12,383,162 B2**
Golestani et al. (45) **Date of Patent: Aug. 12, 2025**

(54) **HUMAN ACTIVITY RECOGNITION USING MAGNETIC INDUCTION-BASED MOTION SIGNALS AND DEEP RECURRENT NEURAL NETWORKS**

(71) Applicant: **UNIVERSITY OF SOUTHERN CALIFORNIA**, Los Angeles, CA (US)

(72) Inventors: **Negar Golestani**, Los Angeles, CA (US); **Mahta Moghaddam**, Los Angeles, CA (US)

(73) Assignee: **University of Southern California**, Los Angeles, CA (US)

(*) Notice: Subject to any disclaimer, the term of this patent is extended or adjusted under 35 U.S.C. 154(b) by 168 days.

(21) Appl. No.: **16/905,735**

(22) Filed: **Jun. 18, 2020**

(65) **Prior Publication Data**

US 2020/0397345 A1 Dec. 24, 2020

Related U.S. Application Data

(60) Provisional application No. 62/863,620, filed on Jun. 19, 2019.

(51) **Int. Cl.**
A61B 5/11 (2006.01)
A61B 5/00 (2006.01)
(Continued)

(52) **U.S. Cl.**
CPC **A61B 5/1118** (2013.01); **A61B 5/002** (2013.01); **A61B 5/0028** (2013.01);
(Continued)

(58) **Field of Classification Search**
CPC A61B 5/1118; A61B 5/002; A61B 5/0028; A61B 5/6823; A61B 5/6824;
(Continued)

(56) **References Cited**

U.S. PATENT DOCUMENTS

8,868,010 B2 * 10/2014 Christensen H03J 1/0008
455/107
9,933,833 B2 * 4/2018 Tu G06F 3/013
(Continued)

FOREIGN PATENT DOCUMENTS

WO WO-2014183275 A1 * 11/2014 .... G06K 9/00362

OTHER PUBLICATIONS

Author: Johari et al., Title: Analysis and Practical Consideration in Implementing Multiple Transmitters for Wireless Power Transfer via Coupled Magnetic Resonance, Date: May 17, 2013, pp. 1774-1783, Publisher: IEEE (Year: 2013).*
Ordoñez et al., Title: Deep Convolutional and LSTM Recurrent Neural Networks for Multimodal Wearable Activity Recognition, Date: Jan. 2016, pp. 1-25 (Year: 2016).*
Cheng, D.K., Field and Wave Electromagnetics, 1983, 515 pgs.
(Continued)

Primary Examiner — Franklin D Balseca
(74) *Attorney, Agent, or Firm* — Brooks Kushman P.C.

(57) **ABSTRACT**

A human activity recognition system includes a receiver coil mounted on a subject and a plurality of transmitter coils mounted on the subject at different locations than the receiver coil and each other. Each transmitter coil is inductively coupled to the receiver coil. A data processing system is in electrical communication with the receiver coil. Characteristically, the data processing system receives signals from each transmitter coils wherein the data processing system applies a machine learning classifier to determine an activity that the subject is engaged in.

19 Claims, 16 Drawing Sheets
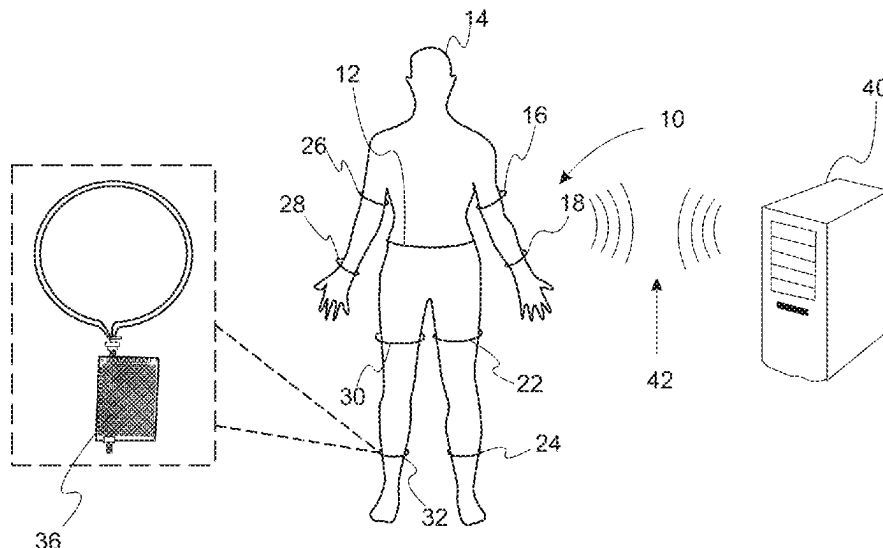
(51) **Int. Cl.**
G06N 3/04 (2023.01)
G06N 3/08 (2023.01)
(52) **U.S. Cl.**
CPC **A61B 5/6823** (2013.01); **A61B 5/6824** (2013.01); **A61B 5/6828** (2013.01); **G06N 3/04** (2013.01); **G06N 3/08** (2013.01)
(58) **Field of Classification Search**
CPC ... A61B 5/6828; A61B 5/1127; A61B 5/0223; A61B 5/11; A61B 5/1114; A61B 5/116; G06N 3/04; G06N 3/08; A61M 2230/00; A61M 2230/63
See application file for complete search history.

(56) **References Cited**

U.S. PATENT DOCUMENTS

10,123,751 B2 *	11/2018	Petterson	A61B 5/7275
10,922,583 B2 *	2/2021	Kaehler	G06N 3/0454
11,194,385 B2 *	12/2021	Chou	H04B 5/02
11,289,953 B2 *	3/2022	Muratov	H02J 7/025
2008/0319349 A1 *	12/2008	Zilberman	A61B 5/0031
			600/587
2015/0375108 A1 *	12/2015	Pathirana	G06F 3/011
			463/39
2020/0029863 A1 *	1/2020	Kiourti	A61B 5/6804

OTHER PUBLICATIONS

Frickey, D.A. et al., "Conversions Between S, Z, Y, h, ABCD, and T Parameters which are Valid for Complex Source and Load Impedances," IEEE Transactions on Microwave Theory and Techniques, v. 42, n. 2 (Feb. 1994), pp. 205-211.

Golestani, N. et al., "Improving the Efficiency of Magnetic Induction-Based Wireless Body Area Network (WBAN)," 2018 IEEE International Microwave Biomedical Conference (IMBioC), Philadelphia, PA, 2018, pp. 166-168, doi: 10.1109/IMBIOC.2018.8428842.

Golestani, N. et al., "Communication System Design for Magnetic Induction-Based Wireless Body Area Network," IEEE 2017, pp. 49-50.

Golestani, N. et al., Theoretical Modeling and Analysis of Magnetic Induction Communication in Wireless Body Area Networks (WBANs), IEEE J. of Electromagnetics, RF, and Microwaves in Medicine and Biology, v. 2, n. 1 (Mar. 2018), pp. 48-55.

Golestani, N. et al., "Human Activity Recognition Using Magnetic Induction-based Motion Signals and Deep Recurrent Neural Networks," Nature Communications 11, 1551 (2020). https://doi.org/10.1038/s41467-020-15086-2.

Ma, Y. et al., "A motion capture library for the study of identity, gender, and emotion perception from biological motion," Behavior Research Methods, 38 (1), (2006), pp. 134-141.

Ofli, F. et al., "Berkeley MHAD: A Comprehensive Multimodal Human Action Database," IEEE 2013, pp. 53.
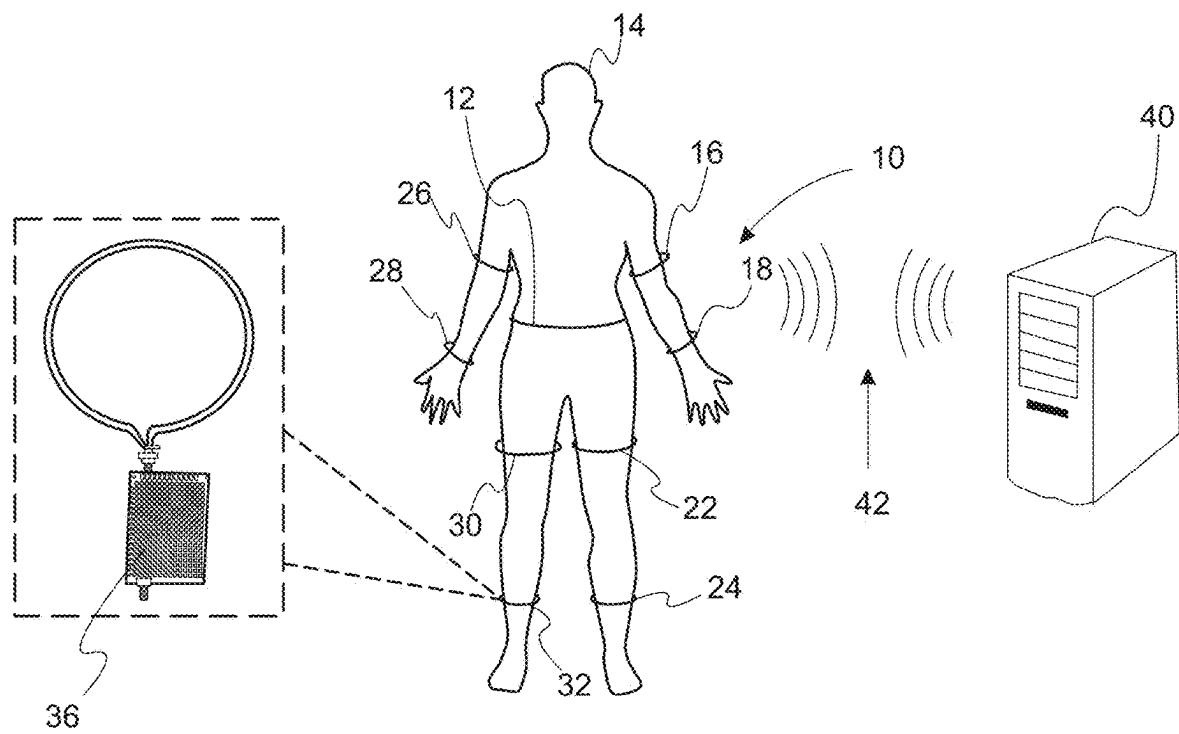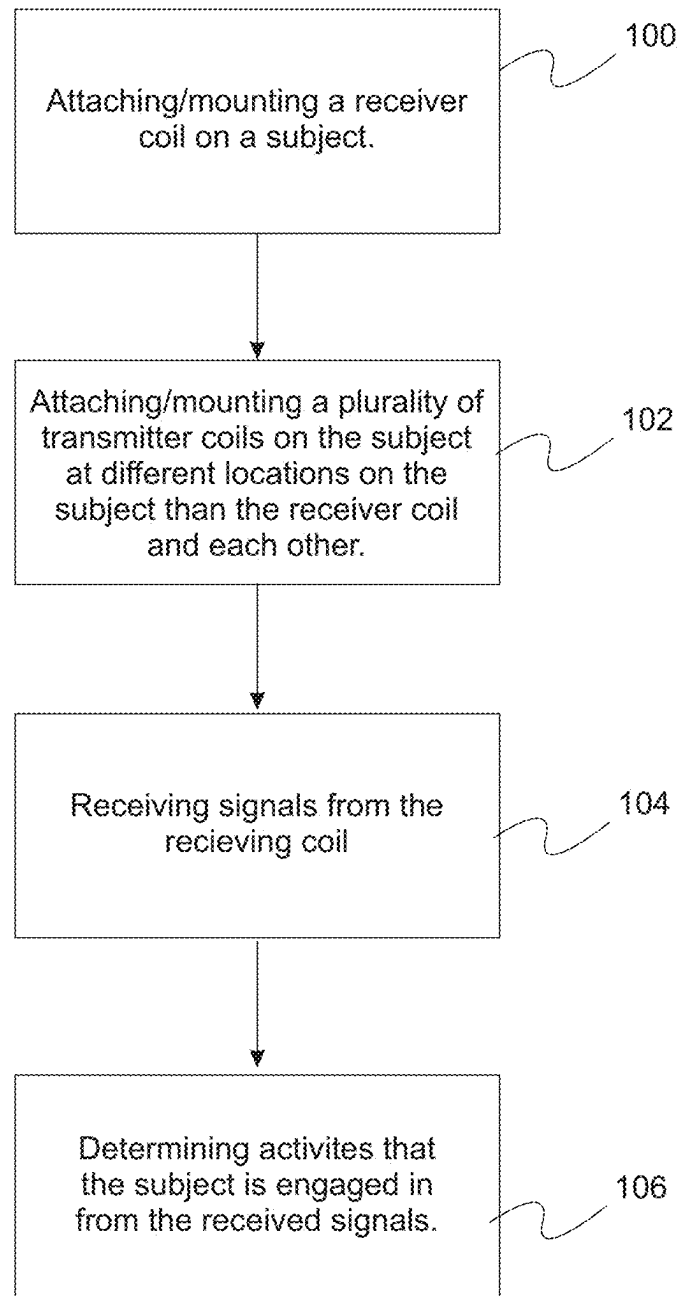
* cited by examiner

Fig. 1A

Attaching/mounting a receiver coil on a subject.

/ 100

Attaching/mounting a plurality of transmitter coils on the subject at different locations on the subject than the receiver coil and each other.

/ 102

Receiving signals from the recieving coil

/ 104

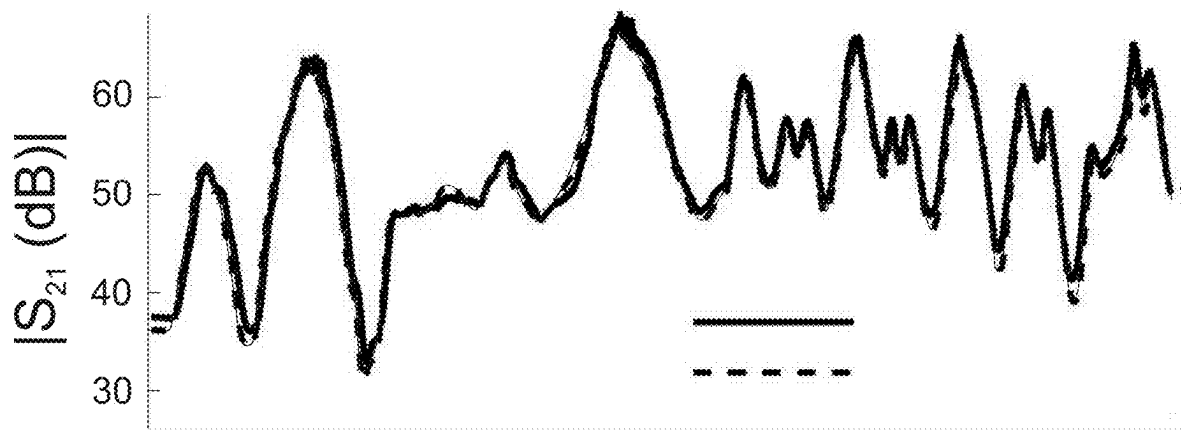Determining activites that the subject is engaged in from the received signals.
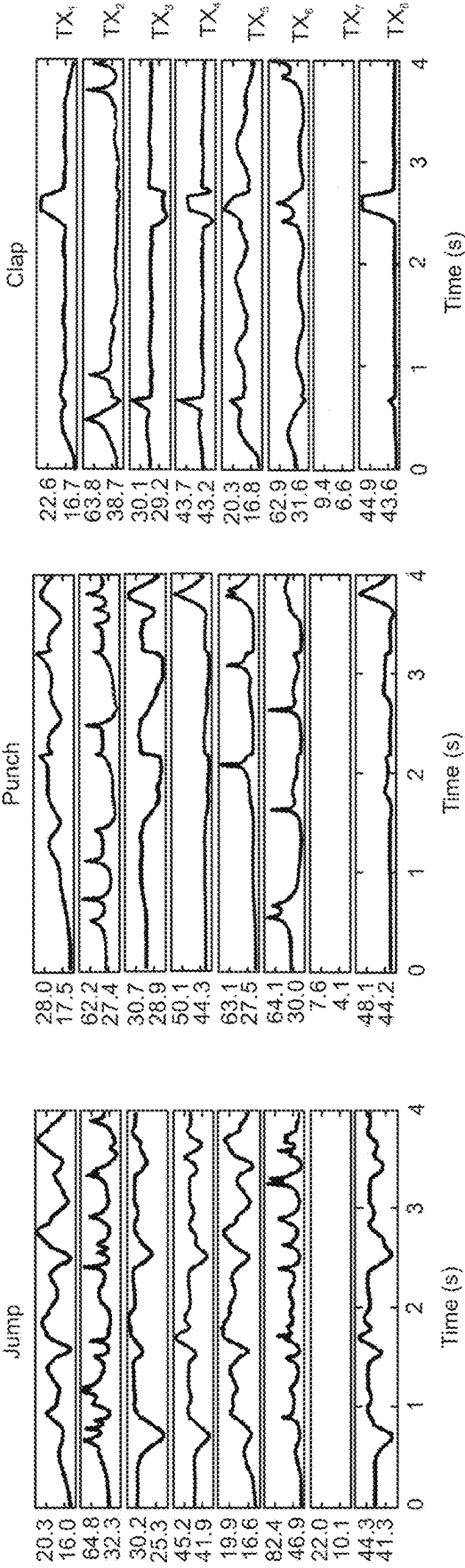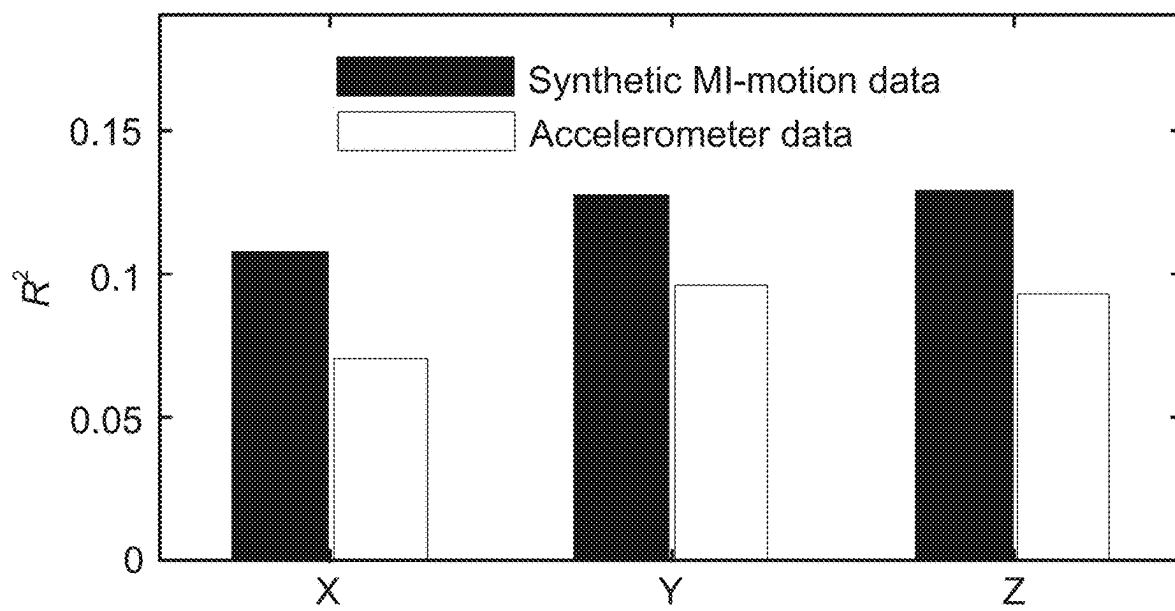
/ 106

Fig. 1B

Fig. 2
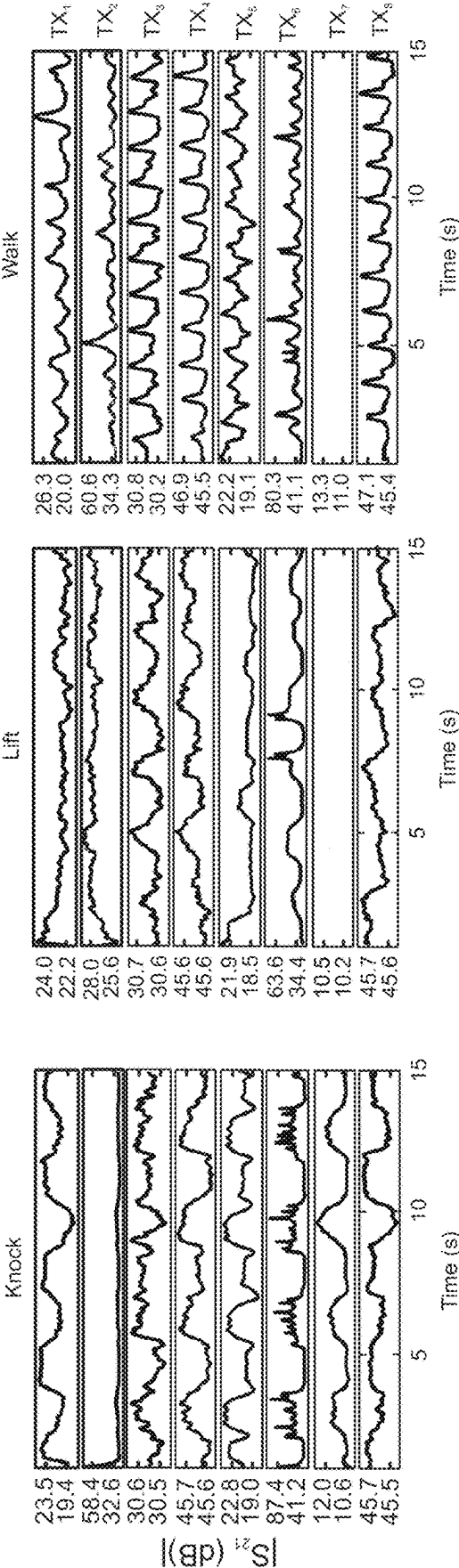
Fig. 3A-3

Fig. 3A-2

Fig. 3A-1

Fig. 3B-3

Fig. 3B-2

Fig.3B-1

Fig. 4

	Knocking	Lifting	Throwing	Walking
Knocking	76.0	4.0	20.0	0.0
Lifting	4.1	71.4	24.5	0.0
Throwing	0.0	13.3	86.7	0.0
Walking	0.0	0.0	0.0	100.0

Fig. 5A

	Knocking	Lifting	Throwing	Walking
Knocking	82.0	6.0	12.0	0.0
Lifting	18.4	49.0	32.7	0.0
Throwing	2.2	11.1	86.7	0.0
Walking	0.0	0.0	0.0	100.0

Fig. 5B

	Knocking	Lifting	Throwing	Walking
Knocking	80.0	6.0	14.0	0.0
Lifting	22.4	55.1	22.4	0.0
Throwing	8.9	17.8	73.3	0.0
Walking	0.0	0.0	0.0	100.0

Fig. 5C

	Knocking	Lifting	Throwing	Walking
Knocking	90.0	6.0	4.0	0.0
Lifting	8.2	71.4	20.4	0.0
Throwing	2.2	13.3	84.4	0.0
Walking	0.0	0.0	0.0	100.0

Fig. 5D

	Knocking	Lifting	Throwing	Walking
Knocking	77.1	4.2	18.8	0.0
Lifting	2.0	67.3	30.6	0.0
Throwing	0.0	9.8	90.2	0.0
Walking	0.0	0.0	0.0	100.0

Fig. 5E

	Knocking	Lifting	Throwing	Walking
Knocking	95.4	3.5	1.0	0.1
Lifting	4.1	74.7	15.0	6.1
Throwing	4.5	14.9	78.7	1.9
Walking	0.0	0.5	0.4	99.0

Fig. 5F

	Jumping	Jumping jacks	Bending	Punching	Waving (two hands)	Waving (one hand)	Clapping	Throwing	Sit-down/stand-up	Sit-down	Stand-up
Jumping	100.0	0.0	0.0	0.0	0.0	0.0	0.0	0.0	0.0	0.0	0.0
Jumping jacks	0.0	100.0	0.0	0.0	0.0	0.0	0.0	0.0	0.0	0.0	0.0
Bending	0.0	0.0	100.0	0.0	0.0	0.0	0.0	0.0	0.0	0.0	0.0
Punching	0.0	0.0	0.0	100.0	0.0	0.0	0.0	0.0	0.0	0.0	0.0
Waving (two hands)	0.0	0.0	0.0	0.0	100.0	0.0	0.0	0.0	0.0	0.0	0.0
Waving (one hand)	0.0	0.0	0.0	0.0	0.0	100.0	0.0	0.0	0.0	0.0	0.0
Clapping	13.3	0.0	0.0	0.0	0.0	0.0	86.7	0.0	0.0	0.0	0.0
Throwing	0.0	0.0	0.0	0.0	0.0	0.0	0.0	100.0	0.0	0.0	0.0
Sit-down/stand-up	0.0	0.0	0.0	0.0	0.0	0.0	0.0	0.0	100.0	0.0	0.0
Sit-down	0.0	0.0	0.0	0.0	0.0	0.0	0.0	0.0	0.0	80.0	20.0
Stand-up	0.0	0.0	0.0	0.0	0.0	0.0	0.0	0.0	0.0	6.7	93.3

Fig. 6A

	Jumping	Jumping jacks	Bending	Punching	Waving (two hands)	Waving (one hand)	Clapping	Throwing	Sit-down/stand-up	Sit-down	Stand-up
Jumping	93.3	0.0	0.0	0.0	0.0	0.0	0.0	6.7	0.0	0.0	0.0
Jumping jacks	0.0	100.0	0.0	0.0	0.0	0.0	0.0	0.0	0.0	0.0	0.0
Bending	0.0	0.0	93.3	0.0	6.7	0.0	0.0	0.0	0.0	0.0	0.0
Punching	0.0	0.0	0.0	100.0	0.0	0.0	0.0	0.0	0.0	0.0	0.0
Waving (two hands)	0.0	0.0	0.0	0.0	73.3	6.7	20.0	0.0	0.0	0.0	0.0
Waving (one hand)	0.0	0.0	0.0	0.0	0.0	86.7	0.0	13.3	0.0	0.0	0.0
Clapping	0.0	0.0	0.0	0.0	0.0	0.0	80.0	6.7	0.0	6.7	6.7
Throwing	0.0	0.0	0.0	0.0	0.0	0.0	6.7	93.3	0.0	0.0	0.0
Sit-down/stand-up	0.0	0.0	6.7	0.0	0.0	0.0	0.0	0.0	93.3	0.0	0.0
Sit-down	0.0	0.0	0.0	0.0	0.0	0.0	0.0	0.0	0.0	80.0	20.0
Stand-up	0.0	0.0	0.0	0.0	0.0	0.0	0.0	0.0	0.0	0.0	100.0

Fig. 6B

|	Jumping	Jumping jacks	Bending	Punching	Waving (two hands)	Waving (one hand)	Clapping	Throwing	Sit-down/stand-up	Sit-down	Stand-up
Jumping	60.0	0.0	6.7	0.0	0.0	0.0	20.0	13.3	0.0	0.0	0.0
Jumping jacks	0.0	93.3	0.0	0.0	0.0	0.0	0.0	6.7	0.0	0.0	0.0
Bending	6.7	0.0	66.7	0.0	13.3	0.0	6.7	6.7	0.0	0.0	0.0
Punching	0.0	0.0	0.0	93.3	0.0	0.0	0.0	6.7	0.0	0.0	0.0
Waving (two hands)	0.0	0.0	0.0	0.0	100.0	0.0	0.0	0.0	0.0	0.0	0.0
Waving (one hand)	0.0	0.0	0.0	0.0	0.0	100.0	0.0	0.0	0.0	0.0	0.0
Clapping	6.7	0.0	0.0	0.0	0.0	0.0	73.3	13.3	0.0	6.7	0.0
Throwing	0.0	0.0	6.7	0.0	6.7	0.0	20.0	66.7	0.0	0.0	0.0
Sit-down/stand-up	0.0	0.0	0.0	0.0	0.0	0.0	0.0	0.0	100.0	0.0	0.0
Sit-down	6.7	0.0	0.0	0.0	0.0	0.0	6.7	0.0	0.0	86.7	0.0
Stand-up	0.0	0.0	0.0	0.0	0.0	0.0	0.0	6.7	0.0	20.0	73.3

Fig. 6C

	Jumping	Jumping jacks	Bending	Punching	Waving (two hands)	Waving (one hand)	Clapping	Throwing	Sit-down/stand-up	Sit-down	Stand-up
Jumping	70.0	0.0	0.0	0.0	0.0	10.0	0.0	10.0	0.0	10.0	0.0
Jumping jacks	0.0	100.0	0.0	0.0	0.0	0.0	0.0	0.0	0.0	0.0	0.0
Bending	0.0	0.0	100.0	0.0	0.0	0.0	0.0	0.0	0.0	0.0	0.0
Punching	0.0	10.0	0.0	90.0	0.0	0.0	0.0	0.0	0.0	0.0	0.0
Waving (two hands)	0.0	0.0	0.0	0.0	100.0	0.0	0.0	0.0	0.0	0.0	0.0
Waving (one hand)	0.0	0.0	0.0	0.0	0.0	100.0	0.0	0.0	0.0	0.0	0.0
Clapping	10.0	0.0	0.0	0.0	0.0	0.0	90.0	0.0	0.0	0.0	0.0
Throwing	0.0	0.0	0.0	0.0	0.0	0.0	0.0	100.0	0.0	0.0	0.0
Sit-down/stand-up	0.0	0.0	0.0	0.0	0.0	0.0	0.0	0.0	100.0	0.0	0.0
Sit-down	0.0	0.0	0.0	0.0	0.0	0.0	10.0	0.0	0.0	90.0	0.0
Stand-up	0.0	10.0	0.0	0.0	0.0	0.0	20.0	0.0	0.0	10.0	60.0

Fig. 6D

	Jumping	Jumping jacks	Bending	Punching	Waving (two hands)	Waving (one hand)	Clapping	Throwing	Sit-down/stand-up	Sit-down	Stand-up
Jumping	80.0	10.0	0.0	0.0	0.0	0.0	10.0	0.0	0.0	0.0	0.0
Jumping jacks	0.0	100.0	0.0	0.0	0.0	0.0	0.0	0.0	0.0	0.0	0.0
Bending	0.0	0.0	100.0	0.0	0.0	0.0	0.0	0.0	0.0	0.0	0.0
Punching	0.0	10.0	0.0	90.0	0.0	0.0	0.0	0.0	0.0	0.0	0.0
Waving (two hands)	0.0	0.0	0.0	0.0	100.0	0.0	0.0	0.0	0.0	0.0	0.0
Waving (one hand)	0.0	0.0	0.0	0.0	0.0	100.0	0.0	0.0	0.0	0.0	0.0
Clapping	10.0	0.0	0.0	0.0	0.0	0.0	80.0	0.0	0.0	10.0	0.0
Throwing	0.0	0.0	0.0	0.0	0.0	10.0	0.0	90.0	0.0	0.0	0.0
Sit-down/stand-up	0.0	0.0	0.0	0.0	0.0	0.0	0.0	0.0	100.0	0.0	0.0
Sit-down	0.0	0.0	0.0	0.0	0.0	0.0	0.0	0.0	0.0	80.0	20.0
Stand-up	0.0	0.0	0.0	0.0	0.0	0.0	0.0	0.0	0.0	20.0	80.0

Fig. 6E

|	Jumping	Jumping jacks	Bending	Punching	Waving (two hands)	Waving (one hand)	Clapping	Throwing	Sit-down/stand-up	Sit-down	Stand-up
Jumping	97.3	0.8	0.0	0.5	0.0	0.0	0.5	0.6	0.0	0.0	0.3
Jumping jacks	0.3	99.7	0.0	0.0	0.0	0.0	0.0	0.0	0.0	0.0	0.0
Bending	0.0	0.5	99.2	0.0	0.3	0.0	0.0	0.0	0.0	0.0	0.0
Punching	0.0	0.0	0.3	99.2	0.0	0.0	0.0	0.5	0.0	0.0	0.0
Waving (two hands)	0.0	0.0	0.0	0.0	100.0	0.0	0.0	0.0	0.0	0.0	0.0
Waving (one hand)	0.0	0.0	0.0	0.0	0.0	100.0	0.0	0.0	0.0	0.0	0.0
Clapping	0.0	0.0	0.0	0.0	0.0	0.0	100.0	0.0	0.0	0.0	0.0
Throwing	0.0	0.0	0.0	0.0	0.0	0.5	0.0	99.5	0.0	0.0	0.0
Sit-down/stand-up	0.0	0.0	0.0	0.0	0.0	0.0	0.0	0.0	96.8	3.2	0.0
Sit-down	0.0	0.0	0.0	0.0	0.0	0.0	0.0	0.0	3.8	96.2	0.0
Stand-up	0.0	0.0	0.0	0.0	0.0	0.0	0.0	0.0	0.0	0.0	100.0

Fig. 6F
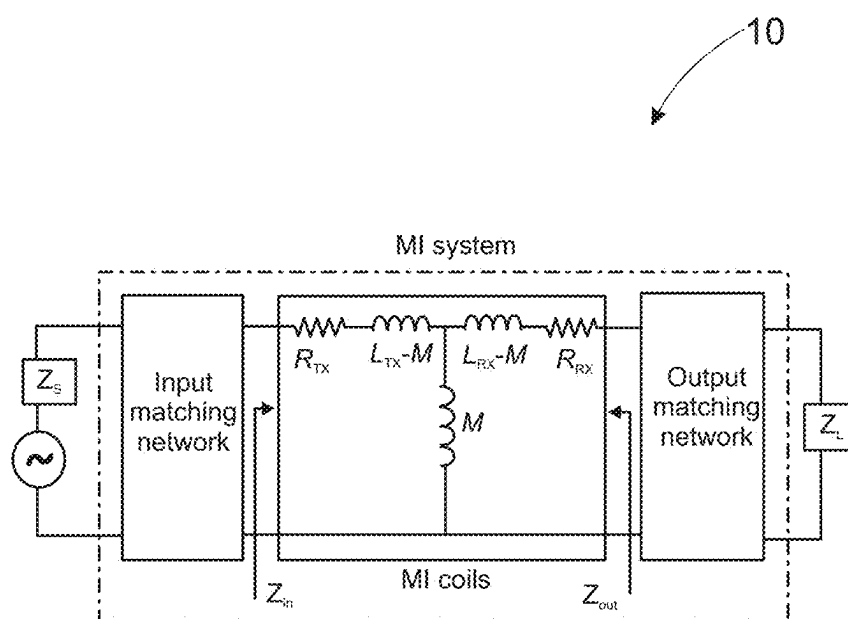
Fig. 7
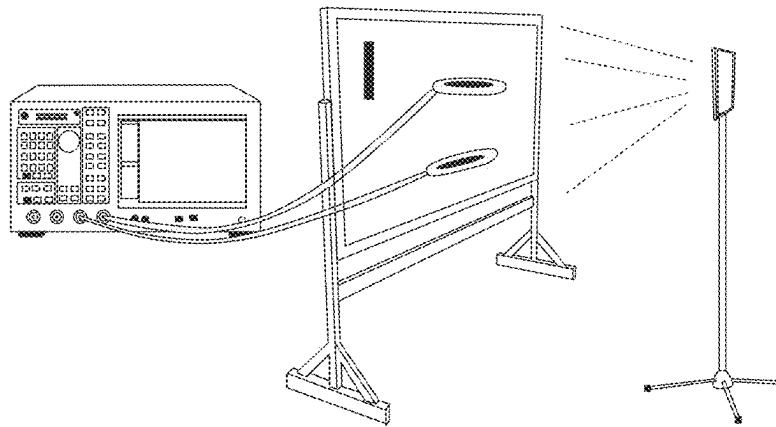
Fig. 8A
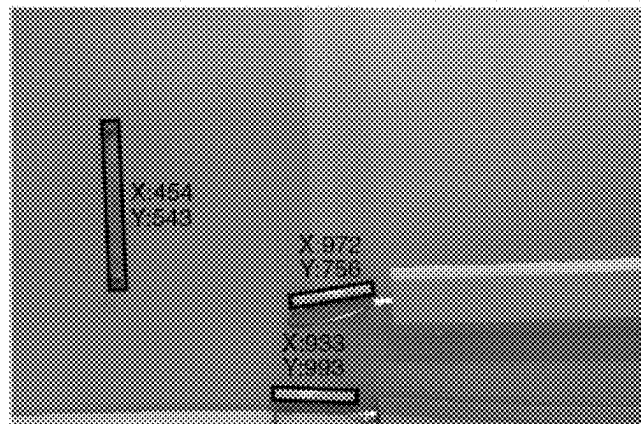
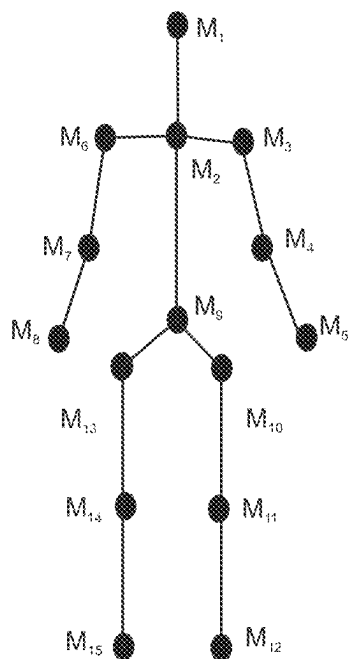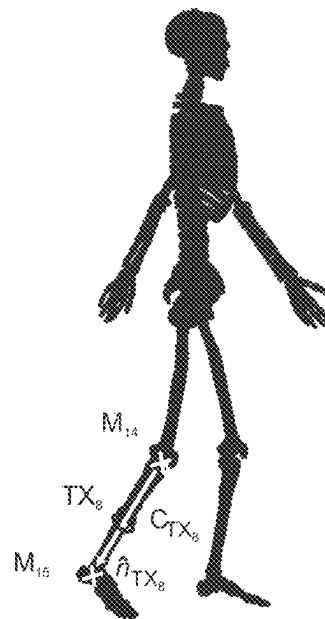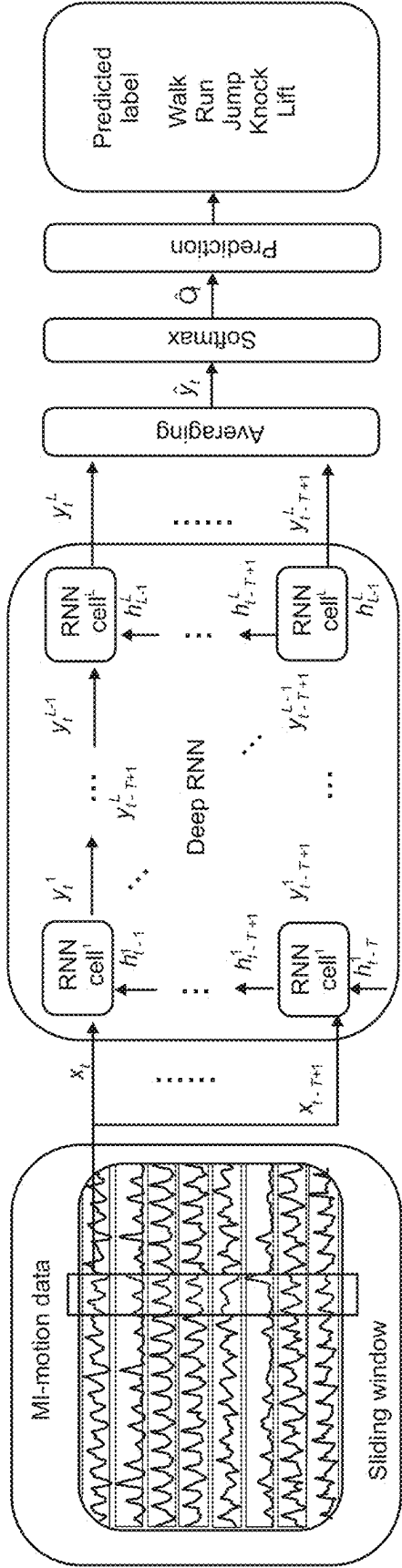*Fig. 8B*
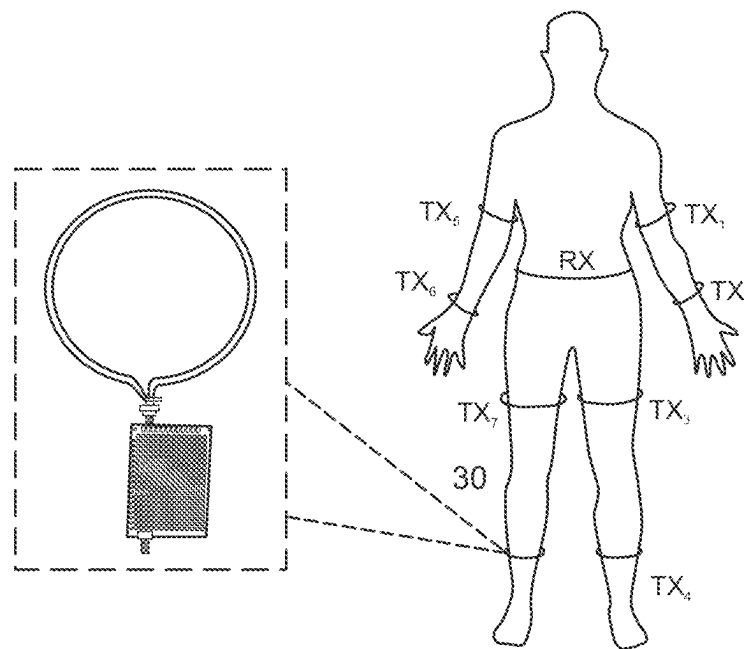
Fig. 9A

Fig. 9B

Fig. 9C

Fig. 10

1

HUMAN ACTIVITY RECOGNITION USING MAGNETIC INDUCTION-BASED MOTION SIGNALS AND DEEP RECURRENT NEURAL NETWORKS

CROSS-REFERENCE TO RELATED APPLICATIONS

This application claims the benefit of U.S. provisional application Ser. No. 62/863,620 filed Jun. 19, 2019, the disclosure of which is hereby incorporated in its entirety by reference herein.

TECHNICAL FIELD

In at least one aspect, the present invention is related to sensor systems for recognizing human activity.

BACKGROUND

Human activity recognition (HAR) aims to provide information on human physical activity and to detect simple or complex actions in a real-world setting. It allows computer systems to assist users with their tasks and to improve the quality of life in areas such as senior care, rehabilitation, daily life-logging, personal fitness, and assistance for people with cognitive disorders[1-6]. Two main approaches for deployment of HAR systems are external and wearable sensors[7]. In the external approach, the monitoring devices are set at fixed points, and users are expected to interact with them[8]. The vision-based technique, for example, is one of the well-known external methods that has been extensively studied for human activity analysis[9, 10]. However, it faces many challenges in terms of coverage, accuracy, privacy, and cost. It requires infrastructure support, such as the installation of video cameras in surveillance areas, which is usually costly. Additionally, cameras cannot capture any data if the user performs out of their reach[11, 12]. In the second approach, on-body sensors, such as accelerometers, gyroscopes, and magnetometers, are used to translate human motion into signal patterns for activity recognition[13-15]. Recent advances in embedded sensor technology have made it feasible to monitor the user's activity using smart devices. Several research studies have reported the use of smartwatches and smartphones in human activity monitoring, and have presented a satisfactory performance[16-19].

Although these devices provide a privacy-aware alternative solution that overcomes many disadvantages of the external approach, they still might not be able to address the requirements of a diverse range of applications. A single wearable cannot cover the entire body and therefore fails to obtain adequate information about the mobility of all body segments[20-22]. For example, inertial sensors embedded in a smartwatch cannot capture the movement of legs, which restricts the capability of the system in classifying activities. Additionally, in systems relying on data from a single device, variations in position can have a significant effect on the performance or lead to the failure of the monitoring system[20,23,24].

Wireless body area network (WBAN) consisting of wearable devices operating around the human body can tackle these problems[21, 25]. In WBANs, sensors are spatially distributed over the human body and collect data from the user. Then data are transmitted wirelessly to a central processing unit for detection. This approach can provide comprehensive information on the mobility of body segments and potentially improve system accuracy. However, WBAN design is

2

challenging as many constraining, and often conflicting, requirements have to be taken into account[26-28]. For example, the system has to be inexpensive, accessible to the general public, and meet ergonomic constraints and health requirements. It has to operate under proper guidelines limiting the power exposure to the user since the energy absorption may lead to temperature elevation in biological tissues. To ensure users' safety, it has to satisfy specific absorption ratio (SAR) constraints, while providing a reliable wireless link[29]. Moreover, the system should guarantee the security and privacy of the user's data. Wearable devices must be small and lightweight, which puts a restriction on the battery size and longevity.

On the other hand, frequent battery recharging may not be practical for sensor networks with multiple sensors in applications such as senior monitoring[7]. Due to the limitation of energy resources, the power management has become a critical issue in designing a WBAN. Since wireless communication consumes a considerable portion of the energy[30], numerous studies have proposed and investigated low-power solutions[31-34]. The conventional state-of-the-art wireless sensor networks working in the vicinity of the human body adopt radio-wave propagation for signal transmission. This technique is susceptible to the characteristics of the environment, and its signal experiences a high attenuation around a lossy medium, such as the human body. It results in higher power consumption, shorter battery life, and lower reliability[33, 35, 36]. Moreover, radio-wave propagation technologies are prone to interference with adjacent communication links since most of them, such as Bluetooth, operate at the busy 2.4 GHz, the industrial, scientific, and medical (ISM) band[37, 38]. They also have potential security problems as their signal cannot be stopped from propagating into free-space. Therefore it can be intercepted even distant from the transmitter[39].

Accordingly, there is a need for improved methods and system for recognizing human activity.

SUMMARY

In at least one aspect, a human activity recognition system includes a receiver coil mounted on a subject and a plurality of transmitter coils mounted on the subject at different locations than the receiver coil and each other. Each transmitter coil is inductively coupled to the receiver coil. A data processing system is in electrical communication with the receiver coil. Characteristically, the data processing system receive signals from each transmitter coils wherein the data processing system apply a machine learning classifier to determine an activity that the subject is engaged in.

In another aspect, a method for determining activities (e.g., physical activities) in a subject is provided. The method includes steps of mounting a receiver coil on the subject and mounting a plurality of transmitter coils on the subject at different locations on the subject than the receiver coil and each other. Received signals are received from the receiver coil wherein a corresponding signal for each transmitter coil in the plurality of transmitter coils is received. The activity or activities that the subject is engaged are determined from the signals.

In another aspect, a magnetic induction-based HAR (MI-HAR) system that effectively detects physical movements by magnetic induction (MI) signals is provided. This system represents the motion of human body parts via variations in the MI signals transmitted from transmitter to the receiver during physical action, instead of spatial data measured by the inertial sensors. Advantageously, this approach over-

comes several problems associated with conventional sensor-based HAR systems, such as eliminating the need for an extra wireless module, reducing power consumption, and the required bandwidth by combining data collection and wireless signal transmission steps. Moreover, it has other features that are inherited from the MI-based communication system. Advantageously, this system is verified for identifying human actions with synthesized MI motion data corresponding to several physical activities. Machine learning-based classifiers and deep recurrent neural networks are applied to classify human movements. The results indicate that the MI signals are informative descriptors for the motion of human body parts.

The foregoing summary is illustrative only and is not intended to be in any way limiting. In addition to the illustrative aspects, embodiments, and features described above, further aspects, embodiments, and features will become apparent by reference to the drawings and the following detailed description.

BRIEF DESCRIPTION OF THE DRAWINGS

For a further understanding of the nature, objects, and advantages of the present disclosure, reference should be had to the following detailed description, read in conjunction with the following drawings, wherein like reference numerals denote like elements and wherein:

FIG. 1A. Schematic of a magnetic induction system.

FIG. 1B. Flowchart of the method implemented by the MI system of claim 1A.

FIG. 2. Measured vs synthetic magnetic induction data. The measured and simulated voltage gain of two MI coils during arbitrary movement, such that both relative alignment and location of coils vary.

FIGS. 3A-1, 3A-2, 3A-3, 3B-1, 3B-2, and 3B-3. Synthetic magnetic induction motion data. The forward voltage gain S_{21} between the receiver (RX) and transmitters (TX$_1$-TX$_8$) are generated using the proposed MI model and the human motion data captured for different activities in two datasets: A) Biological Motion Library (BML) and B) Berkeley Multimodal Human Action Database (MHAD).

FIG. 4. Average R^2 between XYZ of each target point and data of its corresponding accelerometer and magnetic induction (MI) transceiver. The R^2 reports the similarity between two sets of data by a number between zero and one, where a higher number shows a stronger relationship between two datasets.

FIGS. 5A, 5B, 5C, 5D, 5E and 5F. Confusion matrix for the validation set corresponding to the Biological Motion Library (BML). The results correspond to A) support vector machines (SVM), B) K-nearest neighbors (KNN), C) decision trees (DT), D) random forests (RF), E) logistic regression (LR), and F) deep long short-term memory (LSTM) recurrent neural network (RNN) classifiers. The rows and columns represent the percentage of true activity labels and the predicted activity labels, respectively.

FIGS. 6A, 6B, 6C, 6D, 6E, and 6F. Confusion matrix for the validation set corresponding to the Berkeley Multimodal Human Action Database (MHAD). The results correspond to A) support vector machines (SVM), B) K-nearest neighbors (KNN), C) decision trees (DT), D) random forests (RF), E) logistic regression (LR), and F) deep long short-term memory (LSTM) recurrent neural network (RNN) classifiers. The rows and columns represent the percentage of true activity labels and the predicted activity labels, respectively.

FIG. 7. Equivalent two-port network model of magnetic induction (MI) system. The model is integrated with input

and output matching networks, and M, LTX, RTX, LRX, and RRX are the mutual inductance between coils, inductance, and resistance of transmitter and receiver coils, respectively.

FIGS. 8A and 8B. Measurements. a Schematic representation of measurement setup. b The camera frame sample after video processing for object tracking and extracting red and blue markers attached to coils and the fixed-length calibration label, respectively.

FIGS. 9A, 9B, and 9C. Magnetic induction (MI)-based communication system. A) Location of MI transceivers (TX$_i$, RX) on the human body and the laboratory version of an MI transceiver. B) Location of markers (M$_j$) on the body. The marker pairs of (2,9), (3,4), (4,5), (10,11), (11,12), (6,7), (7,8), (13,14), (14,15) define two ends of the torso, left arm, left hand, left thigh, left leg, right arm, right hand, right thigh, and right leg, respectively. Consequently, these pairs can be utilized to calculate the location of coils (C_{TX}, C_{RX}), and their alignment ($\hat{n}_{TX}$, $\hat{n}_{RX}$). C) The center and alignment of a bone and its corresponding coil can be calculated using markers locations.

FIG. 10. Architecture of deep recurrent neural network (RNN). The set of magnetic induction (MI) signals observed by the coils at time t is considered as the input vector x_t. A time window of 1 s (T=1 s) is sliding over the data with 0.5 s overlap, and feeding the truncated subsequences of input data within the window to the batch normalization layer. Then the normalized input data ($x_{t-T+1}, \ldots, x_{t-1}, x_t$) is fetched to the deep long short-term memory (LSTM) model. The network outputs sequences of vectors $y_{t-T+1}^L, \ldots, y_{t-1}^L, y_t^L$, where each output vector shows the prediction score of its corresponding input sample. Assuming the input signals are sequenced to N samples, the overall score of the entire window can be calculated by averaging all of the scores within the window into a single prediction vector of scores by $\hat{y}_t^{70}$. Then the prediction scores are converted into class membership probabilities $\hat{O}_t$ applying a softmax layer. The predicted class membership probability vector contains the probability of every class generated by our model. Then the most probable class is selected as the predicted activity label for the given input data within the time window.

DETAILED DESCRIPTION

Reference will now be made in detail to presently preferred embodiments and methods of the present invention, which constitute the best modes of practicing the invention presently known to the inventors. The Figures are not necessarily to scale. However, it is to be understood that the disclosed embodiments are merely exemplary of the invention that may be embodied in various and alternative forms. Therefore, specific details disclosed herein are not to be interpreted as limiting, but merely as a representative basis for any aspect of the invention and/or as a representative basis for teaching one skilled in the art to variously employ the present invention.

It is also to be understood that this invention is not limited to the specific embodiments and methods described below, as specific components and/or conditions may, of course, vary. Furthermore, the terminology used herein is used only for the purpose of describing particular embodiments of the present invention and is not intended to be limiting in any way.

It must also be noted that, as used in the specification and the appended claims, the singular form "a," "an," and "the" comprise plural referents unless the context clearly indicates otherwise. For example, reference to a component in the singular is intended to comprise a plurality of components.

The term "comprising" is synonymous with "including," "having," "containing," or "characterized by." These terms are inclusive and open-ended and do not exclude additional, unrecited elements or method steps.

The phrase "consisting of" excludes any element, step, or ingredient not specified in the claim. When this phrase appears in a clause of the body of a claim, rather than immediately following the preamble, it limits only the element set forth in that clause; other elements are not excluded from the claim as a whole.

The phrase "consisting essentially of" limits the scope of a claim to the specified materials or steps, plus those that do not materially affect the basic and novel characteristic(s) of the claimed subject matter.

With respect to the terms "comprising," "consisting of," and "consisting essentially of," where one of these three terms is used herein, the presently disclosed and claimed subject matter can include the use of either of the other two terms.

It should also be appreciated that integer ranges explicitly include all intervening integers. For example, the integer range 1-10 explicitly includes 1, 2, 3, 4, 5, 6, 7, 8, 9, and 10. Similarly, the range 1 to 100 includes 1, 2, 3, 4 . . . 97, 98, 99, 100. Similarly, when any range is called for, intervening numbers that are increments of the difference between the upper limit and the lower limit divided by 10 can be taken as alternative upper or lower limits. For example, if the range is 1.1. to 2.1 the following numbers 1.2, 1.3, 1.4, 1.5, 1.6, 1.7, 1.8, 1.9, and 2.0 can be selected as lower or upper limits.

For any device described herein, linear dimensions and angles can be constructed with plus or minus 50 percent of the values indicated rounded to or truncated to two significant figures of the value provided in the examples. In a refinement, linear dimensions and angles can be constructed with plus or minus 30 percent of the values indicated rounded to or truncated to two significant figures of the value provided in the examples. In another refinement, linear dimensions and angles can be constructed with plus or minus 10 percent of the values indicated rounded to or truncated to two significant figures of the value provided in the examples.

The term "connected to" means that the electrical components referred to as connected to are in electrical communication. In a refinement, "connected to" means that the electrical components referred to as connected to are directly wired to each other. In another refinement, "connected to" means that the electrical components communicate wirelessly or by a combination of wired and wirelessly connected components. In another refinement, "connected to" means that one or more additional electrical components are interposed between the electrical components referred to as connected to with an electrical signal from an originating component being processed (e.g., filtered, amplified, modulated, rectified, attenuated, summed, subtracted, etc.) before being received to the component connected thereto.

The term "electrical communication" means that an electrical signal is either directly or indirectly sent from an originating electronic device to a receiving electrical device. Indirect electrical communication can involve processing of the electrical signal, including but not limited to, filtering of the signal, amplification of the signal, rectification of the signal, modulation of the signal, attenuation of the signal, adding of the signal with another signal, subtracting the signal from another signal, subtracting another signal from the signal, and the like. Electrical communication can be

accomplished with wired components, wirelessly connected components, or a combination thereof.

The term "one or more" means "at least one" and the term "at least one" means "one or more." The terms "one or more" and "at least one" include "plurality" as a subset.

The term "substantially," "generally," or "about" may be used herein to describe disclosed or claimed embodiments. The term "substantially" may modify a value or relative characteristic disclosed or claimed in the present disclosure. In such instances, "substantially" may signify that the value or relative characteristic it modifies is within ±0%, 0.1%, 0.5%, 1%, 2%, 3%, 4%, 5% or 10% of the value or relative characteristic.

The term "electrical signal" refers to the electrical output from an electronic device or the electrical input to an electronic device. The electrical signal is characterized by voltage and/or current. The electrical signal can be stationary with respect to time (e.g., a DC signal) or it can vary with respect to time.

The term "electronic component" refers is any physical entity in an electronic device or system used to affect electron states, electron flow, or the electric fields associated with the electrons. Examples of electronic components include, but are not limited to, capacitors, inductors, resistors, thyristors, diodes, transistors, etc. Electronic components can be passive or active. The system described herein, can be implemented with passive transmitters. In this version of the system, the receiver on the waists sends signals to transmitters and receives back the reflected signals. It removes the need for a battery in transmitters and makes them passive.

The term "electronic device" or "system" refers to a physical entity formed from one or more electronic components to perform a predetermined function on an electrical signal.

It should be appreciated that in any figure for electronic devices, a series of electronic components connected by lines (e.g., wires) indicates that such electronic components are in electrical communication with each other. Moreover, when lines directed connect one electronic component to another, these electronic components can be connected to each other as defined above.

The program code embodying the algorithms and/or methodologies described herein is capable of being individually or collectively distributed as a program product in a variety of different forms. The program code may be distributed using a computer-readable storage medium having computer-readable program instructions thereon for causing a processor to carry out aspects of one or more embodiments. Computer-readable storage media, which is inherently non-transitory, may include volatile and non-volatile, and removable and non-removable tangible media implemented in any method or technology for storage of information, such as computer-readable instructions, data structures, program modules, or other data. Computer-readable storage media may further include RAM, ROM, erasable programmable read-only memory (EPROM), electrically erasable programmable read-only memory (EEPROM), flash memory or other solid state memory technology, portable compact disc read-only memory (CD-ROM), or other optical storage, magnetic cassettes, magnetic tape, magnetic disk storage or other magnetic storage devices, or any other medium that can be used to store the desired information and which can be read by a computer. Computer-readable program instructions may be downloaded to a computer, another type of programmable data processing apparatus, or another device from a computer

readable storage medium or to an external computer or external storage device via a network.

Computer readable program instructions stored in a computer-readable medium may be used to direct a computer, other types of programmable data processing apparatus, or other devices to function in a particular manner, such that the instructions stored in the computer-readable medium produce an article of manufacture including instructions that implement the functions, acts, and/or operations specified in the flowcharts or diagrams. In certain alternative embodiments, the functions, acts, and/or operations specified in the flowcharts and diagrams may be re-ordered, processed serially, and/or processed concurrently consistent with one or more embodiments. Moreover, any of the flowcharts and/or diagrams may include more or fewer nodes or blocks than those illustrated consistent with one or more embodiments.

Throughout this application, where publications are referenced, the disclosures of these publications in their entireties are hereby incorporated by reference into this application to more fully describe the state of the art to which this invention pertains.

When a computing device is described as performing an action or method step, it is understood that the computing devices is operable to perform the action or method step typically by executing one or more line of source code. The actions or method steps can be encoded onto non-transitory memory (e.g., hard drives, optical drive, flash drives, and the like).

The term "computing device" refers generally to any device that can perform at least one function, including communicating with another computing device.

The term "subject" refers to a human, mammal, or other animal, including birds and fish as well as all mammals such as primates (particularly higher primates), horses, birds, fish sheep, dogs, rodents, guinea pigs, pig, cat, rabbits, and cows.

Abbreviations

"BML" means biological motion library
"BoW" means bag of word.
"DT" means decision trees.
"DWT" means single-level discrete Wavelet transform.
"FTT" means fast Fourier transform.
"HAR" means human activity recognition.
"ISM" means industrial, scientific, and medical.
"KNN" means k-nearest neighbors algorithm
"LOSO-CV" means leave-one-subject-out cross-validation.
"LR" means logistic regression.
"LSTM" means long short-term memory.
"MHAD" means multimodal human action database.
"MI" means magnetic induction.
"MT-CRBM" means multi-task conditional restricted Boltzmann machines.
"NRMSE" means normalized root-mean-squared error.
"QoS" means quality of service.
"RF" means random forests.
"RX" means receiver.
"TX" means transmitter "RNN" means neural networks.
"SAR" means specific absorption ratio.
"SVM" means support vector machine.
"WBAN" means wireless body area network.

Referring to FIG. 1A, a schematic of an example of a human activity recognition system is provided. Human activity recognition system 10 includes a receiver coil 12 mounted on a subject 14 (e.g., a human) and a plurality of transmitter coils 16-32, mounted on the subject at different

locations on the subject than the receiver coil 12 and each other. Characteristically, each transmitter coil is inductively coupled to the receiver coil 14. A data processing system 40 is in electrical communication with the receiver coil 14. Characteristically, the receiver coil 14 receives signals from each transmitter coils of the plurality of transmitter coils 16-32. Typically, each coil of receiver coil 14 and the plurality of transmitter coils 16-32 include from 1 to 1000 or more turns of a metal wire (e.g., copper wire) of sufficient radius to be positioned around a predetermined body part of the subject. Human activity recognition system 10 operates at frequencies (e.g., has a resonance frequency) less than or equal to about 30 MHZ. For example, the combination of the receiver coil and each transmitter coil will independently have a resonance frequency. In a refinement, the human activity recognition system 10 operates at frequencies from 1 MHz to about 30 MHZ. In a refinement, each of the receiver coil 14 and each transmitter coil in the plurality of transmitter coils 16-32 can be independently attached to a corresponding matching network 36 for each coil.

Data processing system 40 is in electrical communication with receiver coil 14 and receives signals therefrom in order to determine an activity that a subject is engaged in. Typically, data processing 40 includes a computer or other computing device that implements one or more steps of receiving and processing signals from the receiver coil. In a refinement, the data processing system 40 wirelessly communicates with the receiver coil 14 via communication link 42. In another refinement, receiver coil 14 and data processing system 40 are combined into a single electronic device that is mounted on the subject. Advantageously, human activity recognition system 10 can be applied to determine the activities of human subjects for other animals (e.g., mammals). When human activity recognition system 10 is used in veterinary applications, the system can be referred to as an animal activity recognition system.

In a variation, data processing system 40 applies a machine learning classifier to determine an activity that the subject is engaged in. In a refinement, the machine learning classifier is a trained neural network, a support vector machine, non-linear support vector machine with a polynomial kernel, a k-nearest neighbor algorithm, a decision tree, random forests, and logistic regression. In a further refinement, the machine learning classifier is trained to classify received signals into a plurality of predetermined activity classifications. Examples of such activity classifications include, but are not limited to, walking, running, jumping, knocking, lifting, and throwing. In this regard, a trained neural network and in particular, a trained recursive neural network in found to be particularly useful.

In a variation, the receiver coil is mount about a subject's waist. In a refinement, the transmitter coils are mounted on a subject's limbs. In this refinement, the transmitter coils are typically mounted between joints on a subject's limbs. In a refinement, the signals received by the receiver coil are induced signals that are proportional to forward voltage gain.

In still another variation, the data processing system includes a computer operable to execute the trained neural network. In a refinement, the data process system can include a separate interface with another optional computing device that receives the signals from the receiver coil.

Referring to FIG. 1B, a flowchart showing the method implemented by the Human activity recognition system set forth above is provided. In the step depicted by box 100, a receiver coil is mounted on a subject. In box 102, a plurality of transmitter coils are mounted on a subject at different

locations on the subject than the receiver coil and each other. In box **104**, signals are received from the receiver coil wherein a corresponding signal for each transmitter coil in the plurality of transmitter coils is received These signals can be differentiated or multiplexed by techniques known to those skilled in the art. Examples of such techniques include, but are not limited to, Time Division Multiple Access (TDMA) or Frequency Division Multiple Access (FDMA) to differentiate between signals transmitted from transmitters. These aspects can be taken care of with proper communication protocols and packet interface standards. Finally, in box **106**, (physical) activities that the subject is engaged are determined in from the received signal.

Additional details of the invention are set forth in Golestani, N., Moghaddam, M. Author Correction: *Human activity recognition using magnetic induction-based motion signals and deep recurrent neural networks*. Nat Commun 11, 2879 (2020). https://doi.org/10.1038/s41467-020-16581-2; the entire disclosure of which is hereby incorporated by reference.

The following examples illustrate the various embodiments of the present invention. Those skilled in the art will recognize many variations that are within the spirit of the present invention and scope of the claims.

Results

System principle. The MI-based communication system is a short-range wireless physical layer that transmits signals by coupling non-propagating magnetic field between the wire coils rather than radiating as conventional methods. The main component of each node is a coil, which is lightweight, portable, inexpensive, simple, and can be worn as accessories such as belts, wristbands, and jewelry[33, 40]. The manufacturing cost of an MI module is approximately less than $20, while a Bluetooth IMU costs more than $100 (refs. 41-43). The MI coils have a small radiation resistance, which means that the energy propagated to the far-field is negligible. As a result, multipath fading is not an issue, and the MI system can offer a much better quality of service (QoS) compared to Bluetooth-type systems[33, 44, 45]. The non-propagating magnetic field produced by the coils falls off proportional to r^{-3} instead of r^{-1} for radiating fields at a transmission distance r. Although the rapid decay limits the coverage range, it can be favorable in short-range applications such as WBANs46. It allows the signal to remain in a 'bubble' around the coil, which provides a personalized space for the user. It also minimizes the leakage outside the targeted coverage range, reduces interference, increases security, and enables bandwidth reuse[44, 47]. One of the main notable advantages of the MI system is that it works well in lossy dielectric media, such as the human body[48]. In these environments, the MI system experiences much less energy absorption compared to conventional radio-wave propagation technologies[49]. It results in lower SAR for applications working around the human body. Due to smaller path loss, the MI system can transmit a signal with much less power for the same range. This system can be up to six times more efficient in terms of battery power compared to other short-range communication systems (e.g., Bluetooth)[47]. This characteristic enables a large variety of novel and demanding applications in harsh environments such as underwater monitoring of scuba divers[39, 49, 50].

The signal generated by an MI coil attenuates as a function of frequency, channel medium, coils' geometry, location, and alignment (see Methods section)[33]. The non-propagating magnetic field is mainly affected by the perme-

ability of the medium, which is close to the air for non-ferrous materials. The MI channel condition remains constant even in an inhomogeneous lossy medium, such as around the human body[33, 49]. For the frequency of up to 30 MHz, the dimension of the human body is relatively small compared to the wavelength, which makes the propagation and scattering effects insignificant[33]. The immunity of signal in this frequency range to the environment makes the forward voltage gain, S_{21}, of the MI system only a function of coils' locations and alignments for a predefined coil geometry and operating frequency. The gain varies by changing the distance and alignment between the MI coils, and therefore, relative motion between the MI coils yields patterns in the received MI signal. This unique characteristic of the MI system is the fundamental principle of the proposed MI-HAR system.

System framework. The activity recognition process steps are different depending on the application. The framework used in this paper has two main stages: data acquisition and detection. For the first stage, an MI-based communication system is employed, which enables the integration of sensing and wireless data transfer into a single step. The user wears the receiver (RX) coil, for example, as a belt around the waist, and transmitter (TX) coils can be placed around the other skeleton bones, such as wrists, arms, and legs. The human body bones are spatially translated and oriented during a physical activity, which changes the relative location and alignment of the MI coils around them. Collecting the received MI signals transmitted from the coils enclosing skeleton bones can model the relative motion of human bones to represent motion. Since the spatial variations of skeleton bones over time are discriminative descriptors of human actions[51], the vector of samples observed by the MI coils over time can be considered as the set of inputs for the activity detection algorithm. Increasing the number of coils around the skeleton bones results in a broader set of input data. It consequently enhances the accuracy of the MI-HAR system in detecting the relative motion of body parts. In the next step, a classification method is applied to the MI motion data for detecting human action.

MI system setup. The MI transceivers adopted in the experiments consist of a coil and L-reversed impedance matching network[52]. The matching network is used to maximize the transmission efficiency of the overall system[52]. The coils are identical, air-cored, single layer copper with 5 cm radius, 10 AWG wire diameter, and the user can wear them as accessories. The coil's radius can change depending on the size of the body part that they are designed to be placed around. The source and load impedances are 50Ω, and the resonance frequency is 13.56 MHZ. As the operating frequency is lower than 30 MHz, the human body effect is neglected[33], and the effect of the background medium is considered to be the same as that of air. The reversed L-matching networks consist of a series inductor of 5380 nH and a parallel capacitor of 600 pF.

Synthetic MI motion data. In this study, we have synthesized MI motion data to evaluate the proposed MI-HAR system capability in motion detection. The circuit model of the MI system (see Methods section) is used to calculate the forward voltage gain, which is the scaled version of the received MI signal. As the pattern is the same, we used the generated voltage gain patterns of the system as the input features for the detection algorithm. FIG. **1** shows the measured and simulated forward voltage gain of two coils during their movement. Since the distance and misalignment between two coils are required as inputs for the model, their location and alignment are captured using video object

tracking (see Methods section). Results show that the simulated signal is consistent with the measured data, which is an indication of a valid model for generating time-series MI data. We have performed experiments for 20 different motions that involve both geo-translation and misalignment of coils. The average normalized root-mean-squared error (NRMSE) of the synthesized and measured S_{21} for these experiments is less than 10.3%. The reported NRSME not only takes into account model error but also includes the error associated with the motion tracking algorithm using video and vector network analyzer (VNA) measurements.

To synthesize MI motion data during different human actions, we considered a receiver and eight transmitter coils around the torso, hands, arms, legs, and thighs, respectively (see Methods section). For spatial translation and rotation of human body bones, 3D motion capture (MoCap) datasets are employed. Each pair of markers placed at the joints can define a bone. Hence, the location and alignment of MI coils placed around the body parts can be derived and provided as inputs to the model for synthesizing the corresponding MI motion data. Two publicly available experimental datasets: Biological Motion Library (BML)[53] with 4 activities and Berkeley Multimodal Human Action Database (MHAD)[54] with 11 activities are used here. A brief description of these datasets is presented in the Methods section. The generated synthetic forward voltage gain of the MI transceivers corresponds to these datasets is presented in FIG. **3**. A point to consider is that we have extended the single-transmitter/single-receiver model to a multi-transmitter/single-receiver scenario, assuming the interferences such as cross-coupling between coils are negligible, because the interference mitigation techniques such as time-division multiplexing[55] or frequency splitting[56] can be applied to reduce or ideally eliminate interference between inductive systems. Moreover, interference protocols (e.g., RFID interference protocols) can control communication between transceivers while preventing their interference with one other. Therefore, the model can provide a reasonably accurate estimation of multi-coil system performance.

Performance. Tracking the motion of body parts during physical activity is critical in characterizing an individual's movement, and collecting data that provide a more accurate representation of these motions results in better activity detection. The MI signals express a strong relationship with the geo-translation of body segments since the system gain is directly affected by distance and misalignment between coils. Distributing more coils around the human body provides comprehensive information about the user's body movements and results in a better distinction between similar actions. We used the MHAD dataset to compare the capability of the MI signal and accelerometer data in estimating the location of a body part during physical activity. The accelerometer is considered here as a benchmark because it is the most frequently used wearable sensor modality for human activity monitoring. Six markers placed close to the accelerometers are considered as target points. Then the similarity between the 3D location of each target point and data of its corresponding accelerometer and MI transceiver is calculated. We used R^2 as the similarity metric, and the average values over the whole dataset are presented in FIG. **4**. The results show that, on average, the MI signal has a stronger relationship with the 3D location of markers compared to the accelerometer data. This characteristic can be useful not only in classifying human activities but also in reconstructing the motion trajectories of body segments. Many studies have adopted IMUs to reconstruct the trajectories of movements for motion analysis in different appli-

cations. Examples include handwritten digit recognition[57], monitoring trunk kinematics during standing up to sitting down[58], and tracking the motion of body parts on patients who have been affected by neurological conditions for rehabilitation purposes[59]. In inertial sensor-based recognition systems, the velocity and positions are computed indirectly by the integration over sensor measurements. It makes the estimation errors caused by the intrinsic noise/drift grow unbounded with time. For example, the average displacement error of Xsens IMU after 1 min is about 152 m[59]. On the other hand, the MI motion signal is directly affected by the location and orientation of coils. As a result, the trajectory reconstruction using MI signals does not require integration over measured data, which removes the problem of the cumulative error. To assess the performance of the proposed MI-HAR system in recognizing human activities, we implemented deep recurrent neural networks (RNNs) based on long short-term memory (LSTM) units due to their strong performance in human activity detection, and their capability in learning complex representations of the motion data[60,61]. We compared the results of this method with several commonly used classifiers for activity detection using generated synthetic MI motion data. Table 1 summarizes the performance results of LSTM with methods including support vector machines (SVM), K-nearest neighbors (KNN), decision trees (DT), random forests (RF), and logistic regression (LR). The confusion matrix of each classification method on BML and MHAD datasets are also presented in FIGS. **5** and **6**, respectively. The results are compared to other previously introduced methods using different modalities for activity detection. We employed accuracy as an evaluation metric for comparison, as datasets used in this paper are balanced and have an equal number of samples for each activity. The results presented in ref. 62 show that SVM and Multi-Task Conditional Restricted Boltzmann Machines (MT-CRBMs) classifiers have achieved an accuracy of 41.3% and 54.5% using BML motion capture data, respectively. For the MHAD dataset 63, has reported an accuracy of 98% by applying SVM on accelerometer data. The random forest classifier has also achieved an accuracy of 96% and 68.2% using MHAD motion capture and audio data[64]. The accuracy of LSTM using camera RGB image for human activity classification is stated as 92.4% 65. Our results indicate that the deep LSTM model with optimum hyperparameters outperforms other classifiers by a considerable margin on the generated synthetic MI motion data. The recurrent neural networks can capture sequential and time dependencies between input data that results in a strong performance. The LSTM cells let the model capture even longer dependencies compared to vanilla cells. A deep architecture with an optimal number of layers enables the neural network to extract useful discriminative features from the set of input data and to improve the performance of the model. It should be noted that the datasets used in this paper are diverse, which proves the classifier models are valid for a broad range of activity recognition tasks. Moreover, the actions recorded in the BML dataset, including knocking, lifting, and throwing, are very similar as only one hand is moving. The same movement of human body parts in these activities makes it difficult to distinguish and categorize them. Despite these challenges, the deep LSTM model has achieved high accuracy, and it indicates that the recurrent model is capable of classifying human actions by using MI motion signals.

TABLE 1

Performance summary.				
Classifier	Overall	Average	Average	F1 score
BML				
SVM	83.5%	85.4%	83.5%	0.84
KNN	79.4%	80.0%	79.4%	0.8
Decision Trees	77.3%	77.1%	77.1%	0.77
Random Forest	86.6%	86.5%	865%	0.86
Logistic regression	83.5%	86.2%	83.6%	0.85
Deep LSTM	87.0%	86.7%	87.0%	0.87
MHAD				
SVM	96.4%	96.6%	96.4%	0.96
KNN	90.3%	91.1%	90.3%	0.91
Decision Trees	81.2%	82.3%	81.2%	0.82
Random Forest	90.9%	91.8%	90.9%	0.91
Logistic regression	90.9%	91.3%	90.9%	0.91
Deep LSTM	98.9%	98.9%	98.9%	0.99

The result of classification models using generated synthetic magnetic induction (MI) motion data of different datasets.

Discussion

HAR is a powerful technology with a wide range of applications such as healthcare, rehabilitation, sports training, and senior monitoring. We proposed a new wearable-based HAR system using MI for motion capture and wireless signal transmission. This method can tackle existing issues with conventional HAR systems in various aspects, including power consumption, the complexity of implementation, and cost. It can also provide a suitable infrastructure for new applications working in harsh environments, such as underwater. The proposed system is a new sensing approach for capturing human motions, which can also be integrated with other monitoring modalities to provide a more comprehensive HAR system. To show the capability of the MI-HAR system in detecting human movements, we generated synthetic MI motion data received from MI transmitters around the user's body during different activities by the MI system model. As mentioned before, the model used for synthesizing MI motion data does not consider cross-coupling between transmitter coils. However, this cross-coupling is not necessarily destructive and can even provide further information regarding the location and alignment of all coils relative to each other. In this scenario, each received signal is not only a function of the transmitter and receiver coils but also the arrangement of all other coils affects it. Therefore, the movement of even a single body part results in a different signal pattern and can make the system more accurate in detecting actions similar to each other. In the future, we plan to build a realistic deployment-ready prototype of the MI system for capturing MI motion signals during various human activities. Such a system would allow us to perform experiments on real-world MI motion data to demonstrate the accuracy of our method and study the effect of cross-coupling interference on the MI-HAR system. The proposed system can also be integrated with other modalities and monitoring techniques to provide a more comprehensive system for human motion tracking.

We employed several commonly used machine leaning-based classifiers and deep recurrent neural networks for the detection step. We empirically evaluated the proposed MI-HAR system by conducting experiments on the generated synthetic MI motion dataset and discussed the outcomes in detail. Experimental results reveal that the proposed deep

LSTM model shows outstanding performance compared to other approaches. One of the benefits of using the deep recurrent neural network for sequence classification is that it can support multiple parallel temporal input data from different sensor modalities such as MI sensors, accelerometers, and gyroscopes. The model can learn complex features directly from raw data and map them to activities. It removes the need for manual feature engineering by experts while it achieves a comparable performance to models with the feature handcrafting step. Besides, the neural network model enables an interactive learning system when the user provides training data even after the initial training step. It allows the user to fine-tune a pretrained neural network model with their personal data. However, the neural network complexity should be assessed where models have to be implemented in embedded systems with limited processing capability. It highlights the importance of trade-off between computational cost and detection accuracy to ensure real-time feedback.

Methods

Theoretic circuit modeling of the MI system. The MI system consisting of two coils can be modeled as a two-port network shown in FIG. **7**. Coils are attached to impedance matching networks, called input and output matching networks, to maximize the transmission efficiency of the overall system[52]. The closed-form expressions of these circuit parameters are reported in ref 33 to facilitate performance analysis of the MI-based communication system around the human body. The model is validated by simulations and measurements performed for various coils in different locations and alignments relative to each other 33. The average error of all experiments compared with the simulated signal attenuation results is lower than 10% in the frequency range below 30 MHz. The more advanced version of the expressions without any simplification is also calculated and reported in this work.

Assume that the transmitter coil with number of turns N_{TX}, area S_{TX}, and current I_{TX} is centered at C_{TX}, and its surface normal is $\hat{n}_{TX}$. The receiver coil with number of turns N_{RX} and area S_{RX} is centered at C_{RX}, and its surface normal is $\hat{n}_{RX}$. The mutual inductance between the coils in a linear, homogeneous, isotropic background medium with permeability μ and complex propagation constant γ can be calculated from

$$M = \frac{\mu N_{TX}}{I_{TX}} \int_{S_{RX}} H_{TX} \cdot dS_{RX}^{33,66}.$$

By using the exact expressions for the magnetic field generated by the TX coil H_{TX} and applying a procedure similar to ref.[33], one can derive the mutual inductance without any simplification as follows:

$$M = \frac{\mu N_{TX} N_{TX} S_{TX}}{4\pi} \tag{1}$$

$$\int_{\phi'=0}^{2\pi} \int_{\varrho'=0}^{\alpha_{RX}} \rho d\phi d\rho [-\varrho^2 \cos\alpha - \rho\sin\phi(1 + \cos^2\alpha)(c_{rx} \cdot \hat{y}) -$$

$$\rho\sin\phi\sin\alpha\cos\alpha(c_{rx} \cdot \hat{z}) - 2\rho\cos\phi\cos\alpha(c_{rx} \cdot \hat{x}) -$$

$$\cos\alpha(c_{rx} \cdot \hat{x})^2 - \cos\alpha(c_{rx} \cdot \hat{y})^2 - \sin\alpha(c_{rx} \cdot \hat{y})(c_{rx} \cdot \hat{z})] \cdot \mathcal{R}$$

-continued

$$\left\{\frac{1 + \gamma r + \gamma^2 r^2}{r^5}\right\} + [\cos\alpha(c_{rx} \cdot \hat{z})^2 - \sin\alpha(c_{rx} \cdot \hat{z})(c_{rx} \cdot \hat{y}) -$$

$$\rho\sin\phi\sin^2\alpha(c_{rx} \cdot \hat{y}) + \rho\sin\phi\cos\alpha\sin\alpha(c_{rx} \cdot \hat{z})] \cdot \mathcal{R}\left\{\frac{1 + \gamma r}{r^5}e^{-\gamma r}\right\}\right]$$

where r is the distance between the origin and the observation point and can be defined in the cylindrical coordinates as follows:

$$r = r(\rho, \phi) = \tag{2}$$

$$[\rho^2 + (c_{rx} \cdot \hat{x})^2 + (c_{rx} \cdot \hat{y})^2 + (c_{rx} \cdot \hat{z})^2 + 2\rho\sin\phi[\cos\alpha(c_{rx} \cdot \hat{y}) + \sin\alpha(c_{rx} \cdot \hat{z})] + 2\rho\cos\phi(c_{rx} \cdot \hat{x})]^{1/2}$$

The parameters used in the above expressions are calculated from location and alignment of TX/RX coils as follows:

$$\alpha = \tan^{-1}\left(-\frac{\hat{n}_{rx} \cdot \hat{y}}{\hat{n}_{rx} \cdot \hat{z}}\right) \tag{3}$$

$$\hat{n}_{rx} = R_z(\theta_z)R_y(\theta_y)R_x(\theta_x)\hat{n}_{RX} \tag{4}$$

$$C_{rx} = R_z(\theta_z)(R_y(\theta_y)R_x(\theta_x)(C_{RX} - C_{TX}) \tag{5}$$

$$\theta_x = \tan^{-1}\left(-\frac{\hat{n}_{TX} \cdot \hat{y}}{\hat{n}_{TX} \cdot \hat{z}}\right) \tag{6}$$

$$\theta_y = \tan^{-1}\left(-\frac{(\hat{n}_{TX} \cdot \hat{x})}{\sqrt{(\hat{n}_{TX} \cdot \hat{y})^2 + (\hat{n}_{TX} \cdot \hat{z})^2}}\right) \tag{7}$$

$$\theta_z = \tan^{-1}\left(\frac{(\hat{n}_{RX} \cdot \hat{x})[(\hat{n}_{TX} \cdot \hat{y})^2 + (\hat{n}_{TX} \cdot \hat{z})^2]}{(\hat{n}_{RX} \cdot \hat{y})(\hat{n}_{TX} \cdot \hat{z}) - (\hat{n}_{TX} \cdot \hat{y})(\hat{n}_{RX} \cdot \hat{z})} - \left(\frac{(\hat{n}_{TX} \cdot \hat{x})[(\hat{n}_{TX} \cdot \hat{y})^2(\hat{n}_{RX} \cdot \hat{y}) + (\hat{n}_{TX} \cdot \hat{z})(\hat{n}_{RX} \cdot \hat{z})]}{(\hat{n}_{RX} \cdot \hat{y})(\hat{n}_{TX} \cdot \hat{z}) - (\hat{n}_{TX} \cdot \hat{y})(\hat{n}_{RX} \cdot \hat{z})}\right)\right) \tag{8}$$

where $R_x(\theta_x)$, $R_y(\theta_y)$, $R_z(\theta_z)$ are rotation matrices that rotate vectors by an angle θ_x, θ_y, θ_z about the x-, y-, or z-axis using the right-hand rule.

The self-inductance and resistance, which comprises DC resistivity, skin depth δw, and proximity effects, of a coil with radius a, length b, number of turns N, circular cross-section wire, core-material permeability μ, wire diameter ϕ_w, and wire resistivity of ρ_w can be expressed as follows[33, 67]:

$$L = \mu a N^2 \left[\log\frac{8a}{b} - \frac{1}{2} + \frac{b^2}{32a^2}\left(\log\frac{8a}{b} + \frac{1}{4}\right) - \frac{b^4}{1024a^4}\left(\log\frac{8a}{b} - \frac{2}{3}\right) + \frac{10b^6}{131072a^6}\left(\log\frac{8a}{b} - \frac{109}{120}\right) - \frac{35b^8}{4194304a^8}\left(\log\frac{8a}{b} - \frac{431}{420}\right)\right], \tag{9}$$

$$R = \begin{cases} \dfrac{2aN\rho_w}{\delta_w(\phi_w - \delta_w)} & \text{if } \phi_w < \delta_w \\ \dfrac{8aN\rho_w}{\phi_w^2} & \text{if } \phi_w \geq \delta_w \end{cases} \tag{10}$$

There are multiple parameters for analyzing and determining the performance of a two-port network. As the proposed MI-based communication system is a cascaded connection of two-port networks, the ABCD parameters are

the best candidate. These parameters, which are also known as transmission, chain, or cascade parameters, relate the input current and voltage at port-**1** to the output. The ABCD parameters of the MI system are equivalent to the product of ABCD matrices corresponding to the input matching network, the MI system, and the output matching network, accordingly[68]. The scattering matrix S is another set of two-port parameters defined in terms of incident and reflected waves at ports. One of the matrix elements is forward voltage gain S**21**, which shows the voltage of the network at port two divided by the voltage at port-**1**. Converting the ABCD parameters to S-parameters, the forward voltage gain of the MI system can be determined as follows[68]:

$$S_{21} = \frac{2\sqrt{\mathcal{R}\{Z_S\}\mathcal{R}\{Z_L\}}}{AZ_L + B + CZ_SZ_L + DZ_S}, \tag{11}$$

where A, B, C, D are the ABCD parameters of the overall MI system including the MI coils and the matching circuits.

Measurement. The forward voltage gain of two coils is measured for 30 s via a VNA with 1800 points resolution. The corresponding synthetic S21 is also generated by using the system model for comparison. All parameters of the model are predefined based on the MI system setup except the distance and misalignment between coils, which are variable during the movement. Hence, two coils are labeled with red markers and placed in front of a green screen. The motion of coils is captured via an iPhone's built-in camera with 30 fps, and the videos are processed offline to extract markers, their center, and alignment, as shown in FIG. 8. Since only one camera is used, without loss of generality, coils only move in 2D such that the camera can capture their motion. The extracted pixel-wise movement of coils is then converted to the spatial translation using a predefined length 'calibration label'. The ratio of the calibration label's length to its size extracted from video provides a meter to pixel ratio. As the camera is fixed during the experiment, this ratio remains constant for all frames of the video. The recorded distance between coils covers up to 60 cm range. The generated synthetic MI data are synchronized with measured data by minimizing the NRMSE. The code used to track coils and calculate the forward voltage gain of the system based on the circuit model reported in this work is implemented in MATLAB.

Simulation. FIG. **9A** depicts the location of coils considered around the human body for generating synthetic MI motion data. The location of markers required to track coils motion is also displayed in FIG. **9B**. Assuming that the coils are located at the midpoint of bones, we can calculate their center by averaging the location of corresponding paired markers. For example, FIG. **9C** shows the right leg, its corresponding transmitter coil, and markers. The center of the transmitter coil TX$_8$ can be calculated as $c_{TX_8} = (M_{14} + M_{15})/2$. The coils are around the human bones, which indicates that the alignment of the line passing through the

markers is the same as the surface normal of its corresponding coil. Therefore, the surface normal of the transmitter TX_8 can be written as $c_{TX_8}=(M_{14}+M_{15})/|M_{15}+M_{14}|$. The code used to calculate the forward voltage gain of the system based on the circuit model reported in this work is implemented in MATLAB.

Datasets of human activities. The experimental datasets considered in this work contain diverse movement data to verify the applicability of MI-HAR in detecting a wide range of activities. The BML dataset 53 contains a full-body movement dataset for walking, knocking, lifting, and throwing performed by 15 male and 15 female actors in a neutral, angry, happy, and sad style. The dataset is balanced and has the same number of records performed by actors for each action. The total number of samples is 1028, with a sampling rate of 60 Hz. For walking action, the data are captured for 30 s of walking in a triangle turning rightward (clockwise), and turning leftward (counterclockwise). For the knocking, lifting, and throwing actions, five repetitions of a single action unit are obtained for each data record, which is approximately 20 s in duration. The MHAD dataset[54] contains the data for jumping, jumping jacks, bending, punching, waving two hands, waving one hand, clapping, throwing, sit down/stand up, sit down, stand up. The number of records for each action is the same, and each action is performed by seven male and five female subjects, yielding about 659 data sequences. Except for sitting down, stand up, and throwing, all records include five repetitions of a single action. The Data preprocessing. In our experiments, we have used the magnitude of MI signals as input for the classifiers. Data samples are processed before fetching into the classification models. The processing methods are implemented using Python 3.6. For data cleaning, the missing values are substituted with previous non-missing values, and a 5-point quadratic (order 4) polynomial Savitzky-Golay filter is applied for denoising. Then the baseline offset is removed from time-series data. In the MHAD dataset, 3% of the signals are removed from the end of each data sample as the reported experiments show improvement in the accuracy[63].

Classification. The classifier models are implemented using Python 3.6. They are trained and evaluated on the generated synthetic motion datasets of eight bones using the leave-one-subject-out cross-validation (LOSO-CV) method. For the experiments on the BML and MHAD dataset, respectively, six and two subjects are used for validation and the rest for training.

Machine learning-based classifiers: The machine learning-based classifiers are implemented using python library Sklearn[69]. The multi-class models are non-linear SVM with a polynomial kernel, KNN, decision trees, random forests, and logistic regression. We used the bag-of-words (BoW) representation to characterize the time-series data with different lengths. First, the synthetic MI motion data are divided into fixed-length segments of 1 second using the sliding window technique with 0.8 second overlap. Attributes are then computed for the time domain, frequency domain, and time-frequency domain of each window segment. Frequency domain and time-frequency domain representations of the signal are calculated by the fast Fourier transform (FFT), and single-level discrete Wavelet transform (DWT) based on the Daubechies2 wavelet filter, respectively. The attributes considered here are extremes, mean, median, standard deviation, lower quartile, upper quartile, skewness, kurtosis, and the correlation between each pair of signals. As each action is associated with eight data samples, the resulting feature vector for each segment is generated by the concentration of eight feature sets.

Features are also scaled using the min-max scaling method to bound values in the range of 0-1. The scaling makes the weight of all features equal in the process of classification. Next, the feature vectors from the training data are clustered using kmeans clustering to define a codebook that contains the cluster centers, which are called codewords. Then, each window segment is assigned the closest codeword, and a time-series is represented as a histogram of codewords. The bag-of-words representations of synthetic MI motion data are used as inputs for the machine learning-based classification models. In our experiments, we quantized the training data of BML and MHAD datasets to 100 and 20 codewords, respectively.

Recurrent neural network: A schematic diagram of the neural network structure is summarized in FIG. 10. The deep LSTM model is implemented in the TensorFlow framework. We used the mean cross-entropy between the ground truth labels and the predicted class membership probability vector as the loss function, and the network parameters are updated by minimizing this loss function. The model is trained using batch gradient descent with the RMSprop updating rule. In each epoch of training, the entire training set is passed through the neural network model to update the model with an exponentially decaying learning rate. The dropout regularization technique is also applied to all nodes in the network to avoid overfitting. The dropout keep-probability determines the probability of keeping a node during training. After each epoch, the performance of the model is evaluated on the validation set. We evaluated the influence of several hyperparameters related to the network architecture and learning process using grid-search. These hyperparameters and their range of values explored for tuning during training are: number of layers in the range of $\{1, 2, 3, 5, 10\}$, number of units in the range of $\{5, 10, 15, 20, 30, 40, 50\}$, keep probability in the range of $\{0.2, 0.5, 0.8, 1\}$, optimizer decay rate in the range of $\{0.8, 0.85, 0.9, 0.95, 0.98\}$, optimizer momentum in the range of $\{0, 10\text{-}3, 10\text{-}2, 10\text{-}1\}$, initial learning rate in the range of $\{10\text{-}3, 10\text{-}2, 10\text{-}1\}$, exponential decay rate in the range of $\{0.85, 0.9, 0.95, 0.98\}$, and exponential decay step in the range of $\{50, 100, 200, 300\}$. We implemented a five-layer network with 20 and 40 units for BML and MI-IAD datasets, respectively. Both datasets are trained with the optimizer decay rate of 0.95, the initial learning rate of 0.01, the exponential decay rate of 0.98, exponential decay step of 100, and keep the probability of 0.8.

Data Availability

The data that support the findings of this study can be reproduced using the codes developed in this work and are also available on Figshare (https://doi.org/10.6084/m9.figshare.c.4844517). The raw data that our synthetic MI motion data were derived from are available in the public domain: BML dataset (http://paco.psy.gla.ac.uk); MHAD dataset (http://tele-immersion.citris-uc.org/berkeley_mhad); the entire disclosures of which are hereby incorporated by reference.

Code Availability

Computer code supporting the findings of this study are available on GitHub: synthesizing MI data (https://github.com/negargolestani/Synthesize_MI_data); Activity detection (https://github.com/negargolestani/Activity_Detection); the entire disclosures of which are hereby incorporated by reference.

While exemplary embodiments are described above, it is not intended that these embodiments describe all possible forms of the invention. Rather, the words used in the specification are words of description rather than limitation, and it is understood that various changes may be made without departing from the spirit and scope of the invention. Additionally, the features of various implementing embodiments may be combined to form further embodiments of the invention.

REFERENCES

References

1. Yin, J., Yang, Q. & Pan, J. J. Sensor-based abnormal human-activity detection. IEEE Trans. Knowl. Data Eng. 20, 1082-1090 (2008).
2. Kim, J. et al. Wearable smart sensor systems integrated on soft contact lenses for wireless ocular diagnostics. Nat. Commun. 8, 1-8 (2017).
3. Mukhopadhyay, S. C. Wearable sensors for human activity monitoring: a review. IEEE Sens. J. 15, 1321-1330 (2014).
4. Jovanov, E., Milenkovic, A., Otto, C. & De Groen, P. C. A wireless body area network of intelligent motion sensors for computer assisted physical rehabilitation. J. Neuroeng. Rehabil. 2, 6 (2005).
5. Jones, S. E. et al. Genetic studies of accelerometer-based sleep measures yield new insights into human sleep behaviour. Nat. Commun. 10, 1-12 (2019).
6. Kim, J., Campbell, A. S., de Ávila, B. E.-F. & Wang, J. Wearable biosensors for healthcare monitoring. Nat. Biotechnol. 37, 389-406 (2019).
7. Lara, O. D. & Labrador, M. A. A survey on human activity recognition using wearable sensors. IEEE Commun. Surveys Tuts 15, 1192-1209 (2012).
8. Wang, W., Liu, A. X., Shahzad, M., Ling, K. & Lu, S. Understanding and modeling of wifi signal based human activity recognition. In Proc. 21st Annual International Conference on Mobile Computing and Networking, 65-76 (Paris, France, 2015).
9. Poppe, R. A survey on vision-based human action recognition. Image Vis. Comput. 28, 976-990 (2010).
10. Zhang, H.-B. et al. A comprehensive survey of vision-based human action recognition methods. Sensors 19, 1005 (2019).
11. Bodor, R., Jackson, B. & Papanikolopoulos, N. Vision-based human tracking and activity recognition. In 11th Mediterranean Conference on Control and Automation, Vol. 1 (Rhodes, Greece, 2003).
12. Moeslund, T. B., Hilton, A. & Krüger, V. A survey of advances in vision-based human motion capture and analysis. Comput. Vis. Image Und. 104, 90-126 (2006).
13. Kumari, P., Mathew, L. & Syal, P. Increasing trend of wearables and multimodal interface for human activity monitoring: a review. Biosens. Bioelectron. 90, 298-307 (2017).
14. Hua, A. et al. Accelerometer-based predictive models of fall risk in older women: a pilot study. NPJ Digit. Med. 1, 1-8 (2018).
15. Nweke, H. F., Teh, Y. W., Al-Garadi, M. A. & Alo, U. R. Deep learning algorithms for human activity recognition using mobile and wearable sensor networks: State of the art and research challenges. Expert Syst. Appl. 105, 233-261 (2018).
16. Lu, Y. et al. Towards unsupervised physical activity recognition using smartphone accelerometers. Multimed. Tools Appl. 76, 10701-10719 (2017).
17. Cvetković, B., Szeklicki, R., Janko, V., Lutomski, P. & Luštrek, M. Real-time activity monitoring with a wristband and a smartphone. Inf. Fusion 43, 77-93 (2018).
18. Hassan, M. M., Uddin, M. Z., Mohamed, A. & Almogren, A. A robust human activity recognition system using smartphone sensors and deep learning. Future Gener. Comp. Syst. 81, 307-313 (2018).
19. Wang, J., Chen, Y., Hao, S., Peng, X. & Hu, L. Deep learning for sensor-based activity recognition: a survey. Pattern Recogn. Lett. 119, 3-11 (2019).
20. Allahbakhshi, H., Hinrichs, T., Huang, H. & Weibel, R. The key factors in physical activity type detection using real-life data: a systematic review. Front. Physiol. 10, 75 (2019).
21. Gao, L., Bourke, A. & Nelson, J. Evaluation of accelerometer based multisensor versus single-sensor activity recognition systems. Med. Eng. Phys. 36, 779-785 (2014).
22. Chen, L., Hoey, J., Nugent, C. D., Cook, D. J. & Yu, Z. Sensor-based activity recognition. IEEE Trans. Syst., Man, Cybern. Syst. 42, 790-808 (2012).
23. Sztyler, T., Stuckenschmidt, H. & Petrich, W. Position-aware activity recognition with wearable devices. Pervasive Mob. Comput. 38, 281-295 (2017).
24. Cornacchia, M., Ozcan, K., Zheng, Y. & Velipasalar, S. A survey on activity detection and classification using wearable sensors. IEEE Sens. J. 17,386-403 (2016).
25. Ertuğrul, Ö. F. & Kaya, Y. Determining the optimal number of body-worn sensors for human activity recognition. Soft Comput. 21,5053-5060 (2017).
26. Sharma, S., Tripathi, M. & Mishra, V. Survey paper on sensors for body area network in health care. In International Conference on Emerging Trends in Computing and Communication Technologies (ICETCCT), 1-6 (IEEE, Dehradun, India, 2017).
27. Mosenia, A., Sur-Kolay, S., Raghunathan, A. & Jha, N. K. Wearable medical sensor-based system design: a survey. IEEE Trans. Multi-Scale Comput. Syst. 3,124-138 (2017).
28. Gravina, R., Alinia, P., Ghasemzadeh, H. & Fortino, G. Multi-sensor fusion in body sensor networks: state-of-the-art and research challenges. Inf. Fusion 35,68-80 (2017).
29. Movassaghi, S., Abolhasan, M., Lipman, J., Smith, D. & Jamalipour, A. Wireless body area networks: a survey. IEEE Commun. Surveys Tuts. 16,1658-1686 (2014).
30. Aroganam, G., Manivannan, N. & Harrison, D. Review on wearable technology sensors used in consumer sport applications. Sensors 19,1983 (2019).
31. Cavallari, R., Martelli, F., Rosini, R., Buratti, C. & Verdone, R. A survey on wireless body area networks: technologies and design challenges. IEEE Commun. Surv. Tuts 16, 1635-1657 (2014).
32. Negra, R., Jemili, I. & Belghith, A. Wireless body area networks: applications and technologies. Procedia Comput. Sci. 83,1274-1281 (2016).
33. Golestani, N. & Moghaddam, M. Theoretical modeling and analysis of magnetic induction communication in wireless body area networks (wban). IEEE J. Electromagn. RF Microw. Med. Biol. 2,48-55 (2018).
34. Hasan, K., Biswas, K., Ahmed, K., Nafi, N. S. & Islam, M. S. A comprehensive review of wireless body area network. J. Netw. Comput. Appl. 143, 178-198 (2019).
35. Bae, J., Cho, H., Song, K., Lee, H. & Yoo, H.-J. The signal transmission mechanism on the surface of human

body for body channel communication. IEEE Trans. Microw. Theory Techn. 60, 582-593 (2012).

36. Werner, D. H. & Jiang, Z. H. Electromagnetics of Body Area Networks: Antennas, Propagation, and RF Systems (John Wiley and Sons, 2016).

37. Hayajneh, T., Almashaqbeh, G., Ullah, S. & Vasilakos, A. V. A survey of wireless technologies coexistence in wban: analysis and open research issues. Wirel. Netw. 20, 2165-2199 (2014).

38. Natarajan, R., Zand, P. & Nabi, M. Analysis of coexistence between IEEE 802.15. 4, BLE and IEEE 802.11 in the 2.4 GHz ISM band. In IECON 2016—42nd Annual Conference of the IEEE Industrial Electronics Society, 6025-6032 (IEEE, Florence, Italy, 2016).

39. Sharma, A. K. et al. Magnetic induction-based non-conventional media communications: a review. IEEE Sens. J. 17, 926-940 (2016).

40. Golestani, N. & Moghaddam, M. Communication system design for magnetic induction-based wireless body area network. In USNC-URSI Radio Science Meeting (Joint with AP-S Symposium), 49-50 (IEEE, 2017).

41. Vicon. https://www.vicon.com/hardware/blue-trident. Accessed 29 Jan. 2020.

42. Zenshin Technology. https://zenshin-tech.com. Accessed 29 Jan. 2020.

43. Prayudi, I. & Kim, D. Design and implementation of imu-based human arm motion capture system. In IEEE International Conference on Mechatronics and Automation, 670-675 (IEEE, Chengdu, China, 2012).

44. Tal, N., Morag, Y., Shatz, L. & Levron, Y. Design optimization of transmitting antennas for weakly coupled magnetic induction communication systems. PLoS ONE 12, e0171982 (2017).

45. Bansal, R. Near-field magnetic communication. IEEE Antennas Propag. Mag.

46. 114-115 (2004). 46. Sun, Z. & Akyildiz, I. F. Magnetic induction communications for wireless underground sensor networks. IEEE Trans. Antennas Propag. 58,2426-2435 (2010).

47. Agbinya, J. I. & Masihpour, M. Power equations and capacity performance of magnetic induction communication systems. Wirel. Pers. Commun. 64,831-845 (2012).

48. Sun, Z., Akyildiz, I. F., Kisseleff, S. & Gerstacker, W. Increasing the capacity of magnetic induction communications in rf-challenged environments. IEEE Trans. Commun. 61,3943-3952 (2013).

49. Kim, H.-J. et al. Review of near-field wireless power and communication for biomedical applications. IEEE Access 5,21264-21285 (2017).

50. Domingo, M. C. Magnetic induction for underwater wireless communication networks. IEEE Trans. Antenn. Propag. 60,2929-2939 (2012).

51. Vemulapalli, R., Arrate, F. & Chellappa, R. Human action recognition by representing 3d skeletons as points in a lie group. In Proc. IEEE Conference on Computer Vision and Pattern Recognition, 588-595 (Columbus, Ohio, 2014).

52. Golestani, N. & Moghaddam, M. Improving the efficiency of magnetic induction-based wireless body area network. In IEEE International Microwave Biomedical Conference (IMBioC), 166-168 (IEEE, Philadelphia, Pennsylvania, 2018).

53. Ma, Y., Paterson, H. M. & Pollick, F. E. A motion capture library for the study of identity, gender, and emotion perception from biological motion. Behav. Res. Methods 38,134-141 (2006).

54. Ofli, F., Chaudhry, R., Kurillo, G., Vidal, R. & Bajcsy, R. Berkeley mhad: a comprehensive multimodal human action database. In IEEE Workshop on Applications of Computer Vision (WACV), 53-60 (IEEE, Tampa, Florida, 2013).

55. Johari, R., Krogmeier, J. V. & Love, D. J. Analysis and practical considerations in implementing multiple transmitters for wireless power transfer via coupled magnetic resonance. IEEE Trans. Ind. Electron. 61,1774-1783 (2013).

56. Cannon, B. L., Hoburg, J. F., Stancil, D. D. & Goldstein, S. C. Magnetic resonant coupling as a potential means for wireless power transfer to multiple small receivers. IEEE Trans. Power Electron 24,1819-1825 (2009).

57. Pan, T.-Y., Kuo, C.-H., Liu, H.-T. & Hu, M.-C. Handwriting trajectory reconstruction using low-cost imu. IEEE Trans. Emerg. Top. Comput. Intell. 3,261-270 (2018).

58. Giansanti, D., Maccioni, G., Benvenuti, F. & Macellari, V. Inertial measurement units furnish accurate trunk trajectory reconstruction of the sitto-stand manoeuvre in healthy subjects. Med. Biol. Eng. Comput. 45,969-976 (2007).

59. Suvorova, S., Vaithianathan, T. & Caelli, T. Action trajectory reconstruction from inertial sensor measurements. In 11th International Conference on Information Science, Signal Processing and their Applications (IS-SPA), 989-994 (IEEE, Montreal, Quebec, 2012).

60. Ordóñez, F. J. & Roggen, D. Deep convolutional and lstm recurrent neural networks for multimodal wearable activity recognition. Sensors 16,115 (2016).

61. Hammerla, N. Y., Halloran, S. & Plotz, T. Deep, convolutional, and recurrent models for human activity recognition using wearables. In 25th Int. Joint Conf. Artif. Intell. (IJCAI), 1533-1540 (New York, New York, 2016).

62. Shields, T. J., Amer, M. R., Ehrlich, M. & Tamrakar, A. Action-affectgender classification using multi-task representation learning. In IEEE Conference on Computer Vision and Pattern Recognition Workshops (CVPRW), 2249-2258 (IEEE, Honolulu, Hawaii, 2017).

63. Mimouna, A., Khalifa, A. B. & Amara, N. E. B. Human action recognition using triaxial accelerometer data: selective approach. In 15th International Multi-Conference on Systems, Signals and Devices (SSD), 491-496 (IEEE, Hammamet, Tunisia, 2018).

64. Garcia-Ceja, E., Galván-Tejada, C. E. & Brena, R. Multi-view stacking for activity recognition with sound and accelerometer data. Inf. Fusion 40, 45-56 (2018).

65. Noori, F. M., Wallace, B., Uddin, M. Z. & Torresen, J. A robust human activity recognition approach using openpose, motion features, and deep recurrent neural network. In Scandinavian Conference on Image Analysis, 299-310 (Springer, Norrköping, Sweden, 2019).

66. Cheng, D. K. et al. Field and Wave Electromagnetics. Pearson Education India (Addison-Wesley, 1989).

67. Rosa, E. B. Calculation of the Self-Inductance of Single-Layer Coils. 31 (US Government Printing Office, 1906).

68. Frickey, D. A. Conversions between s, z, y, h, abcd, and t parameters which are valid for complex source and load impedances. IEEE Trans. Microw. Theory Techn. 42, 205-211 (1994).

69. Pedregosa, F. et al. Scikit-learn: Machine learning in python. J. Mach. Learn. Res. 12, 2825-2830 (2011).

70. Murad, A. & Pyun, J.-Y. Deep recurrent neural networks for human activity recognition. Sensors 17, 2556 (2017).

What is claimed is:

1. A human activity recognition system comprising: a receiver coil mounted on a subject;

    a plurality of transmitter coils mounted on the subject at different locations than the receiver coil and each other wherein each transmitter coil is inductively coupled to the receiver coil such that the receiver coil receives signals from the plurality of transmitter coils, the receiver coil and each transmitter coil having a sufficient radius to be positioned around a predetermined body part of the subject, wherein the transmitter coils are coupled to the receiver coil with a non-propagating magnetic field; and

    a data processing system in electrical communication with the receiver coil, the data processing system receiving the signals from each of the transmitter coils wherein the data processing system applies a machine learning classifier to determine an activity that the subject is engaged in, wherein multiplexing or frequency splitting is applied to reduce or eliminate interference between inductive systems and wherein each of the receiver coil and each transmitter coil in the plurality of transmitter coils are independently attached to a corresponding matching network for each coil, wherein the machine learning classifier is specifically trained to classify received signals into a plurality of predetermined activity classifications including walking, running, jumping, knocking, lifting, and throwing, wherein a combination of the receiver coil and each transmitter coil has an operating frequency from 1 to 30 MHZ and wherein data collection and wireless signal transmission are combined.

2. The human activity recognition system of claim 1 wherein the data processing system wirelessly communicates with the receiver coil.

3. The human activity recognition system of claim 1 wherein the data processing system is combined with the receiver coil.

4. The human activity recognition system of claim 1 wherein the machine learning classifier is a trained neural network, a support vector machine, a non-linear support vector machine with a polynomial kernel, a k-nearest neighbors algorithm, a decision tree, a random forest, and logistic regression.

5. The human activity recognition system of claim 1 wherein the machine learning classifier is a trained neural network.

6. The human activity recognition system of claim 1 wherein the receiver coil is mounted about a subject's waist.

7. The human activity recognition system of claim 6 wherein the transmitter coils are mounted on a subject's limbs.

8. The human activity recognition system of claim 6 wherein the transmitter coils are mounted between joints on a subject's limbs.

9. The human activity recognition system of claim 6 wherein the signals received by the receiver coil are forward voltage gains.

10. The human activity recognition system of claim 1 wherein the data processing system includes a computing device operable to execute the machine learning classifier.

11. A method for determining activities in a subject, the method comprising:

    mounting a receiver coil on the subject;

    mounting a plurality of transmitter coils on the subject at different locations on the subject than the receiver coil and each other, the receiver coil and each transmitter coil having a sufficient radius to be positioned around a predetermined body part of the subject, wherein the transmitter coils are coupled to the receiver coil with a non-propagating magnetic field;

    receiving signals from the receiver coil wherein a corresponding signal for each transmitter coil in the plurality of transmitter coils is received; and

    determining the activities that the subject is engaged by a machine learning classifier from the signals received from the receiver coil, the machine learning classifier being specifically trained to classify received signals into a plurality of predetermined activity classifications including walking, running, jumping, knocking, lifting, and throwing, wherein multiplexing or frequency splitting is applied to reduce or eliminate interference between inductive systems and wherein each of the receiver coil and each transmitter coil in the plurality of transmitter coils are independently attached to a corresponding matching network for each coil, wherein a combination of the receiver coil and each transmitter coil has an operating frequency from 1 to 30 MHZ and wherein data collection and wireless signal transmission are combined.

12. The human activity recognition system of claim 1 wherein the subject is a human or mammal.

13. The human activity recognition system of claim 1 wherein the receiver coil is configured to be worn as a belt worn about a subject's waist.

14. The human activity recognition system of claim 1 wherein the receiver coil and each transmitter coil in the plurality of transmitter coils are independently attached to a corresponding L-reversed impedance matching network.

15. The human activity recognition system of claim 14 the machine learning classifier, distinguishes human activities by capturing sequential and time dependencies between the signals from the plurality of transmitter coils.

16. The human activity recognition system of claim 1 wherein the signals received by the receiver coil are induced signals that are proportional to forward voltage gain, and the data processing system applies a deep long short-term memory (LSTM) recurrent neural network as the machine learning classifier to determine the activity that the subject is engaged in, based on the induced signals.

17. The method of claim 11, wherein the machine learning classifier is a trained neural network, a support vector machine, a non-linear support vector machine with a polynomial kernel, a k-nearest neighbors algorithm, a decision tree, a random forest algorithm, or a logistic regression.

18. The method of claim 11, wherein the machine learning classifier is a trained neural network.

19. The method of claim 11 wherein the receiver coil is mounted about a subject's waist and the transmitter coils are mounted on a subject's limbs.

* * * * *